CONFIDENTIAL

UNCLASSIFIED

RM-L53F17

Copy 182

RM L53F17

NACA

RESEARCH MEMORANDUM

CANCELLED

Classification

CHANGED TO *Unclassified*

By authority of *naca Research Abs #9*

Changed by *man* Date *11-9-55*

METHOD OF ESTIMATING THE INCOMPRESSIBLE-FLOW PRESSURE

DISTRIBUTION OF COMPRESSOR BLADE SECTIONS

AT DESIGN ANGLE OF ATTACK

By John R. Erwin and Laura A. Yacobi

Langley Aeronautical Laboratory
Langley Field, Va.

NATIONAL ADVISORY COMMITTEE
FOR AERONAUTICS

WASHINGTON
December 9, 1953

CONFIDENTIAL

UNCLASSIFIED

UNCLASSIFIED

NATIONAL ADVISORY COMMITTEE FOR AERONAUTICS

RESEARCH MEMORANDUM

METHOD OF ESTIMATING THE INCOMPRESSIBLE-FLOW PRESSURE

DISTRIBUTION OF COMPRESSOR BLADE SECTIONS

AT DESIGN ANGLE OF ATTACK

By John R. Erwin and Laura A. Yacobi

SUMMARY

A method was devised to estimate the incompressible-flow surface pressures of compressor airfoils in cascade at design angle of attack by modifying the known pressure distribution of the section as an isolated airfoil. In this method, the incremental velocities due to camber and thickness are assumed proportional to the average stream velocity through the blade passage. The incremental velocities are further modified by the use of interference factors determined from a systematic study of cascade test results with NACA 65-series compressor blade sections. Comparisons were made between estimated and experimental pressure distributions of the NACA 65-(12)10 section in cascade over a range of solidities and inlet angles. The estimated pressure distributions of NACA 65-series sections of other cambers and thicknesses were compared with test results. Good agreement was obtained.

To determine whether the interference factors obtained from 65-series sections of constant mean-line loading could be applied to other types of compressor blades, comparisons between estimated and experimental pressure distributions of sections having loading concentrated near the trailing edge and sections with leading-edge loading were made. Good agreement was obtained, so that the method is believed to have general application.

INTRODUCTION

The aerodynamic requirements for axial-flow compressors for aircraft gas turbines are high specific flow capacity, high pressure ratio per stage, and high efficiency. To fulfill the first two of these demands, the flow must enter the blade rows at high speeds. Blades having significant camber appear to be required. To achieve high efficiency, optimum combinations of section thickness, thickness distribution, camber, camber

distribution, solidity, and angle of attack should be selected for various radial stations of each blade row. The minimum passage areas within the blade rows must be sufficiently large to prevent choking of the flow. The surface Mach numbers and the surface pressure gradients must be kept below limiting values to prevent extensive separation of the boundary layers. Also, from structural considerations axial-flow compressor blades must have sufficient strength to resist flutter and vibration and to prevent breaking under combined centrifugal and aerodynamic loads.

In selecting the optimum thickness distribution and mean line for a compressor blade section, a knowledge of the pressures that would occur over the blade surfaces in incompressible flow is desirable. This information is of use in estimating how much the velocity of the flow will increase from the entering conditions to the minimum-pressure region on the blade surface. The entrance Mach number associated with the first occurrence of sonic velocity or some other limiting value of local velocity can then be estimated with a degree of accuracy sufficient for comparative purposes. Further, the pressure gradients the boundary layer will encounter can be examined to estimate whether separation of the flow is likely.

Previously, pressures over compressor blade surfaces have been obtained theoretically for nonviscous flow. The differences between ideal flows and actual flows are large in many cases (ref. 1). Due to the many variables involved, no experimental program could be expected to include all the possible combinations that arise during the design of a multistage compressor. A simple method of estimating the pressures over the surfaces of compressor blade sections would provide useful information concerning blade sections other than those investigated experimentally. Such a method would thus be a desirable complement to experimental investigations.

The approach employed in the present investigation was to modify the known characteristics of isolated airfoils (see ref. 2; for example) to the conditions that occur in cascade. The incremental surface velocities due to camber and thickness were assumed to be proportional to the average velocity through the cascade. The interference between adjacent airfoils was examined as a function of several significant cascade and section parameters. The intent of this investigation was to determine whether the variation of the interference was systematic and, if so, to devise a simple method having general application of estimating the incompressible-flow pressure distributions about airfoils in cascade.

This report presents a simple method of estimating the pressures over the surfaces of compressor blade sections in cascade at design angle of attack for viscous, incompressible, two-dimensional flow. Interference factors proportional to the solidity, camber, and inlet

air angle of the cascade were derived from experimental results. Comparisons between estimated and experimental pressure distributions were made over a range of solidities, inlet air angles, and cambers for two types of mean lines.

SYMBOLS

C_{l_0} camber, expressed as design isolated-airfoil lift coefficient

F interference factor

F_0 general interference factor

F_1 interference factor applying to the unconfined region AB (see fig. 2)

F_2 interference factor applying to the region CF (see fig. 2)

P total pressure

P_R resultant pressure coefficient; difference between local upper- and lower-surface pressure coefficients

p static pressure

q dynamic pressure

S pressure coefficient, $\dfrac{P_1 - p_l}{q_1}$

V velocity

Δv_α incremental velocity due to angle of attack

Δv_c incremental velocity due to camber

Δv_t incremental velocity due to thickness

α angle of attack (see fig. 1)

β air angle measured from axis of compressor (see fig. 1)

σ solidity, ratio of blade chord to spacing

Subscripts:

1   upstream of cascade

2   downstream of cascade

l local

av   average

DISCUSSION OF METHOD

General

The incremental velocities over the surfaces of isolated airfoils can be considered to be due to separate effects of camber, thickness, and angle of attack. Values for these effects, proportional to the free-stream velocity, are presented in reference 2 for a wide range of basic sections and mean lines. To a good order of approximation, the incremental velocities can be added directly to the free-stream velocity to obtain the resultant surface velocities.

When airfoils are placed in compressor cascade arrangement, the free-stream velocities upstream and downstream of the airfoils are no longer equal in magnitude or direction as in the case of isolated airfoils. Therefore, the surface velocities of airfoils in cascade are quite different from the velocities over the same section in a free stream. To estimate the velocity distribution over an airfoil in cascade, it appears possible that the known velocity distribution about the isolated airfoil could be modified in a manner related to the variation of the average stream velocity through the cascade.

The velocity at a point on the surface of an airfoil in cascade is, however, affected by other factors besides the average stream velocity at that chordwise station in the cascade. The interference of the adjacent airfoils must be considered. The interference between airfoils at design angle of attack is a function of the cascade parameters of solidity, inlet angle, and Mach number (not considered herein), and the section parameters of thickness and camber in both distribution and magnitude. Examination of pressure distributions over the surfaces of a series of related compressor blade sections in cascade (ref. 3) indicated that the variation of the interference with certain of these parameters appeared to be systematic. The purpose of this investigation was to determine whether the variation of the interference was systematic and, if so, to devise a simple method of estimating the incompressible-flow pressure distributions about airfoils in cascade.

For this preliminary study, attention will be concentrated on esti-
mating pressure distributions of axial-flow compressor blade sections
operating at design angle of attack. Design angle of attack is assumed
to be that angle for which there is no contribution of angle of attack
to the surface pressures. An indication that the effect of the angle of
attack can be systematized was contained in reference 4. In the refer-
ence paper, a linear relation was observed between the incremental veloci-
ties and the angle of attack for the particular sections investigated.

Concept of Flow

In figure 2, streamlines and equipotential lines for potential flow
through a typical cascade of compressor blade sections are illustrated.
This wire-mesh plot was obtained by the methods of reference 5. In this
analysis, the flow through a cascade of airfoils is considered in several
steps. Far upstream the effect of individual blades is insignificant.
As the flow approaches the cascade, the presence of individual blades is
felt and the flow must deviate from a straight path to accommodate the
thickness and curvature of the sections. It was assumed that no net
change in pressure or direction occurs, however, until the flow enters
the blade row; that is, until the flow is within the area defined by the
axial projection of the blades (area between dashed lines in fig. 2). In
the region AB of figure 2, then, the interference of the adjacent blades
is small. As the flow enters the blade row, changes in pressure and
direction of the flow occur. In the region BC the flow is not confined
by solid boundaries but a change in flow properties from the upstream con-
ditions to those within the solid boundaries of region CD must occur. In
the confined passage, region CD, the maximum interference between blades
occurs. The regions DE and EF are, respectively, similar to the regions
BC and AB concerning net changes in pressure and direction. Downstream
of the cascade the flow becomes uniform in static pressure and direction.

Average stream velocity.- The velocity at the blade surface is con-
sidered to be the sum of the average stream velocity and the incremental
velocities due to section camber and thickness. (The effects of angle of
attack are important when off-design operation is considered but are neg-
lected in the present investigation.) The incremental velocities are
considered to be proportional to the average stream velocity. The method
used to determine the value of the average stream velocity at any chord-
wise station through a cascade is as follows. In the region AB, no net
change in static pressure was assumed to occur so the average stream veloc-
ity is taken equal to the upstream velocity. In the confined region CD,
the average stream velocity for a two-dimensional passage is determined
by the distance between blades. This distance is taken along a potential
line. The change in average velocity in the transition region BC is
assumed to occur smoothly. Similar treatment is applied to obtain the
variation of average velocity in the chordwise direction at the exit from
the cascade.

The ideal exit velocity is easily calculated for a given cascade if the inlet angle and turning angle are known. The inlet angle is assumed to be a known quantity in this analysis. The experimental investigation reported in reference 6 indicated that compressor cascades differing only in camber distribution produced essentially the same turning angle. Therefore, if the camber of a section is known, the turning angle at design angle of attack can be closely estimated from the results presented in reference 3. This estimate can be checked by comparing the lift coefficient obtained by integrating the calculated pressure distribution with the lift coefficient associated with the estimated turning angle. The actual exit velocity will be different from the ideal because of the boundary layers. The magnitude of the difference can be estimated from figure 87 of reference 3.

Interference factors.- Using the local value of average stream velocity rather than the upstream velocity to compute the surface velocity accounts for the diffusion or expansion that occurs through a cascade. In addition, the influence of adjacent airfoils must be considered. To consider the effect exactly for a range of the several cascade and section parameters would be extremely tedious. The simplifying assumption was made that one interference factor would apply in region AB and another would apply in region CD, with a smooth transition in between for a given cascade configuration. In order to reduce the extent of this investigation, the interference factor determined for region CD was assumed to apply to regions DE and EF.

The formula for the surface pressure coefficient S for an isolated airfoil in incompressible fluid is given in reference 2 in terms of v, the velocity over the basic thickness form at zero angle of attack, and Δv and Δv_α, the incremental velocities due to the camber of the mean line and due to the angle of attack, respectively:

$$ S = \left(\frac{v}{V} \pm \frac{\Delta v}{V} \pm \frac{\Delta v_\alpha}{V} \right)^2 \tag{1} $$

In this equation, the local velocities and increments are referred to the free-stream velocity V which is constant upstream and downstream. From equation (1), an expression for the local velocity referred to the upstream velocity V_1 may be written

$$ \frac{V_l}{V_1} = S^{1/2} = 1 + \frac{\Delta v_t}{V_1} \pm \frac{\Delta v_c}{V_1} \pm \frac{\Delta v_\alpha}{V_1} \tag{2} $$

For flow in cascade, the incremental velocities due to thickness, camber, and angle of attack are assumed to be proportional to the average passage velocity at any chordwise station V_{av}:

$$\Delta v_t' = F \; \Delta v_t \; \frac{V_{av}}{V_1} \tag{3a}$$

$$\Delta v_c' = F \; \Delta v_c \; \frac{V_{av}}{V_1} \tag{3b}$$

$$\Delta v_\alpha' = F \; \Delta v_\alpha \; \frac{V_{av}}{V_1} \tag{3c}$$

where F is the cascade interference factor and primed values refer to the cascade.

Further, the local velocity is assumed to be the sum of the average passage velocity and the several incremental velocities:

$$\frac{V_l}{V_1} = \frac{V_{av}}{V_1}\left(1 + \frac{\Delta v_t'}{V_{av}} \pm \frac{\Delta v_c'}{V_{av}} \pm \frac{\Delta v_\alpha'}{V_{av}}\right) \tag{4}$$

Substituting equation (3) into equation (4) results in

$$\frac{V_l}{V_1} = \frac{V_{av}}{V_1}\left[1 + F\left(\frac{\Delta v_t}{V_1} \pm \frac{\Delta v_c}{V_1} \pm \frac{\Delta v_\alpha}{V_1}\right)\right] \tag{5}$$

Neglecting the incremental velocities due to angle of attack Δv_α, combining the terms in parentheses to a simpler notation $\Delta v_l/V_1$, and solving for the interference factor yields

$$F = \frac{1}{\Delta v_l/V_1}\left(\frac{V_l/V_1}{V_{av}/V_1} - 1\right) \tag{6}$$

Knowing experimental values of V_l/V_1, theoretical values of $\Delta v_l/V_1$ from reference 2, and V_{av}/V_1 from the passage width through a cascade, values of the interference factor can be determined directly.

DETERMINATION OF AVERAGE PASSAGE VELOCITY

The variation of the average velocity through a cascade for the incompressible-flow case can be found directly if the passage area at suitable chordwise stations is known. The distribution of passage area can be measured directly from a suitably scaled drawing of two adjacent blades. At any chordwise station, the passage width is the length of a line everywhere normal to the streamlines. The position of such an equipotential line can be approximated with sufficient accuracy in most cases by a circular arc normal to the bounding surface on each side of the passage. Aids have been devised for estimating the location of an equipotential line rapidly. One aid, the locator, consists of a thin sheet of transparent plastic inscribed with a series of circular arcs tangent to each other at one point which is considered as the origin (fig. 3). A line normal to the arcs is passed through this point. To simplify measurement of the arc lengths, 1-inch intervals are marked on each arc, starting from the origin. The interval marks can be connected by faired curves to provide a continuous indication of points of equal curvilinear distance from the origin.

To obtain the width of a passage at any chordwise station, the locator is placed over a drawing of the passage. The straight line is positioned tangent to the surface with the origin at the desired chordwise station (fig. 3(b)). The circular arc that is normal to the opposite surface of the passage is ascertained. A second aid, the planchette, is a small square of transparent plastic having two lines inscribed at right angles. For convenience, a scale marked in 0.05-inch intervals is inscribed along one of the perpendicular lines, starting at the intersection of the lines. The lines inscribed at right angles on the planchette are helpful in selecting the proper arc or in interpolating between arcs.

The ratio of the average passage velocity to the entering velocity is then found as the ratio of the distance between adjacent stagnation streamlines far upstream of the cascade to the length of the equipotential line measured within the cascade. This procedure is carried out for both surfaces within the region of the passage confined by the blade surfaces. To obtain values of the average velocity in the unconfined regions BC and DE, faired curves representing the variation of velocity with distance along the chord are drawn from the values obtained by measurement to the entering and leaving velocities.

EXPERIMENTAL DATA

Some experimental data not previously published have been included in this study. These data were obtained in low-speed cascade tunnels at the Langley Laboratory. The NACA 65-010 section was tested at several solidities with blades of unit aspect ratio for $\beta = 0°$ in the 5-inch cascade tunnel (ref. 3). The NACA 65-(12)10 and 63-(12A$_4$K$_6$)06 sections (see appendix) were tested in a similar 10-inch cascade tunnel at $\sigma = 1.0$ and 1.5 for $\beta = 0°$ with blades of aspect ratio 2.

DERIVATION OF INTERFERENCE FACTORS

General

The factors affecting the interference between airfoils in cascade considered in this study are solidity, inlet angle, section thickness, and camber. The experimental data available were taken primarily from NACA 65-series compressor blade sections. The interference between blades is believed to be influenced more by the physical position of one airfoil with respect to another and by the thickness and camber of the sections than by the particular type of mean line or thickness distribution used. It is therefore believed that, if a systematic variation of factors can be found for one type of compressor blade section, the same system will apply to the general case of airfoils in cascade. Sections having other mean lines and thickness distributions are examined subsequently to substantiate this belief.

Influence of Solidity

Zero inlet angle.- One of the primary factors affecting the interference between airfoils in cascade is the solidity. In order to isolate the effects of solidity to permit direct evaluation, data for the NACA 65-010 compressor blade section at zero angle of attack and zero inlet angle for solidities of 0.5, 0.75, 1.0, 1.25, and 1.50 were analyzed. As a first step, the variation of the surface velocity at the 40-percent-chord station was plotted as a function of solidity. The average stream velocity across the passage at the 40-percent-chord station was also plotted as a function of solidity. These relations, presented in figure 4, indicate that the surface velocity does not increase as rapidly with solidity as does the average velocity. From equation (6), values of the interference factor at zero inlet angle for the various solidities were obtained (fig. 4). An equation fitting this curve and satisfying the isolated-airfoil condition $F_0 = 1.0$ at $\sigma = 0$ was found:

$$F_0 = 1 - \left(0.576\sigma - 0.140\sigma^2\right) \tag{7}$$

The relation between F and solidity was derived by using values taken at the 40-percent-chord station. To ascertain that this same factor applied to other chordwise stations, the chordwise distribution of S was computed for the NACA 65-010 section at solidities of 0.5, 0.75, 1.0, and 1.5. Comparison of the computed and test values of S for these solidities (fig. 5) indicates excellent agreement except for regions of laminar separation. Further, the pressure distribution about NACA 65-(12)10 compressor blade sections at a solidity of 1.0 and design angle of attack was calculated by using the appropriate interference factor for this solidity (fig. 6). The excellent agreement obtained between calculated and test values indicates that the interference at zero inlet angle is not affected by the amount of the camber of the sections and thus can have general application.

Inlet angles of 45° and 60°.- In order to determine the effect of solidity on the interference factors at inlet angles other than zero, the NACA 65-(12)10 compressor blade was examined at solidities of 0.5, 0.75, 1.0, and 1.5 for inlet angles of 45° and 60°. Layouts of two blades were made for each condition with the sections drawn at the appropriate design angle of attack. The variation of average velocity through each passage was obtained by the previously described method. (As a confined passage is not formed by adjacent blades for the lowest solidity at $\beta = 45°$, or at $\sigma = 0.5$ and 0.75 for $\beta = 60°$, the average velocity beyond the entrance region AB could not be determined from the drawings. These low-solidity conditions required a different treatment that is described in a later section.) Knowing experimental values of local velocity, theoretical values of incremental velocity due to camber and thickness, and the average passage velocity, interference factors for the regions AB and CF were computed from equation (6). The 15-percent-chord station of the convex surface was considered typical for region AB, and the 90-percent-chord station on the concave surface typical for region CF. Values of F_1 and F_2 were examined as functions of solidity for the two inlet angles. An equation fitting the curve of F_1 against solidity and satisfying the isolated airfoil condition was found:

$$F_1 = 1 - KL\left(1.15\sigma^{0.71} - 0.15\sigma^3\right) \tag{8}$$

where K is a function of inlet angle and L is a function of camber.

The factor F_2 used for the confined-passage region CD and for the concave surface was found to vary with solidity at $\beta = 45°$ and 60° in a manner similar to that in which F_0 varied at $\beta = 0°$, although the

magnitudes were lower. Thus, the relation between interference and solidity obtained at zero inlet angle could be applied to the confined passage of other cascade combinations when modified for the effects of inlet angle and camber:

$$F_2 = MN(F_0) = MN(1 - 0.576\sigma + 0.140\sigma^2) \tag{9}$$

where M is a function of inlet angle and N is a function of camber.

Values of the interference factors obtained from equations (8) and (9) and the appropriate constant for the product of KL and MN for each inlet angle were used to calculate pressure distributions about NACA 65-(12)10 compressor blade sections for $\sigma = 0.75$, 1.0, and 1.5 at $\beta = 45^{\circ}$ and for $\sigma = 1.0$ and 1.5 at $\beta = 60^{\circ}$. Comparison of the calculated pressure distributions with cascade test data (fig. 7) indicates generally good agreement. For $\beta = 45^{\circ}$ and $\sigma = 1.5$, however, the values of S computed at 30 and 40 percent chord for the convex surface, indicated by crosses, were in error and were neglected in fairing. This error probably results from the method used in selecting the extent of the regions to which F_1 and F_2 apply. As the system worked well for other combinations of β and σ, no attempt to modify the method for this particular combination was made.

The values of average passage velocity and interference factor used in estimating the pressure distributions presented in figure 7 are shown in figure 8. The extent of the dashed portions of the curves indicates the fairing used between known values. In fairing the average-velocity curves, the trend of the known values was used to select the extent and shape of the faired portions. The interference-factor curves were drawn as straight lines between points A and B, B and C, and C and D (fig. 2). The lines were faired for a distance of 10 percent chord on both sides of the resulting intersections.

Influence of Inlet Angle

The chordwise position of adjacent blades has a significant effect on the interference between blades. At constant solidity, the chordwise position is determined by the values of the inlet angle and the angle of attack. The intent of this preliminary analysis is to evolve methods of estimating the surface pressures at design angle of attack so that only the effects of inlet angle will be considered. Experimental data for the NACA 65-(12)10 section at unit solidity and inlet angles of 0°, 30°, 45°, 60°, and 70° were used in this study.

The values of the interference factor F_1 for the region AB and the interference factor F_2 for the region CF, for the several inlet angles for which test data were available, were plotted as a function of inlet angle. The values used were averages of the regions represented rather than values for a particular chordwise station. As the local velocities in the leading-edge region are very sensitive to angle of attack, precise values of F_1 at design angle of attack could not be determined.

At constant solidity, the terms containing σ in equations (8) and (9) remain constant. Since the camber was held constant in this study, L and N in equations (8) and (9) also remain constant. Since KL and MN appear as products in these equations, any desired value can be assigned to L and N for the conditions being examined. Therefore, L and N were assigned unit value for $C_{l_0} = 1.2$. Equations (8) and (9) could then be evaluated directly to obtain values of K and M. An equation fitting the curve of F_1 as a function of inlet angle at unity solidity and a camber of 1.2 was obtained and solved for K:

$$K = 0.08 + 0.45 \sin \beta \tag{10}$$

An equation fitting the curve of F_2 as a function of inlet angle at unit solidity and a camber of 1.2 was obtained and solved for M:

$$M = 1 - 0.62 \sin^2\beta \tag{11}$$

Values for the interference factors obtained from these equations were used to compute the pressure distribution about NACA 65-(12)10 compressor blade sections for inlet angles of 0°, 30°, 45°, 60°, and 70° at unit solidity. In figure 9, the calculated pressure distributions are compared with test data taken at angles of attack near design. For the convex surface, the agreement is very good for all inlet angles except $\beta = 70^\circ$. At $\beta = 70^\circ$, the calculated values are lower and less peaked than the test values over the forward region. The value of F_1 required and the region to which F_1 would have to be applied in order to yield exact agreement are not in line with the trends indicated at other inlet angles. To avoid further complexity, the present method was not altered to improve the agreement at this condition. For the concave surface, the agreement between experimental and computed values is generally good, although a tendency for the calculated values to be low is apparent. Some of the difference shown is due to laminar separation over the concave surface. Equation (11) is believed to yield results of sufficient accuracy for most purposes when applied to the convex surface in the enclosed-passage region and to the entire concave surface.

Effect of Camber

From equation (6), values of the interference factor were computed for compressor blades of several cambers to discern the effects of camber. The NACA 65-010, 65-410, 65-(12)10, 65-(18)10 and 65-(24)10 sections at $\beta = 45°$ and $\sigma = 1.0$ were used. For the uncambered section, no correction appeared to be necessary for the unconfined region AB. For the confined-passage region CD and for the "concave" surface of the 65-010 blade, no adjustment other than F_0, the correction for solidity found at $\beta = 0$, was required. The values of L in equation (8) required for the cambered sections were found to follow the relationship

$$L = 0.97C_{l_o}{}^{0.2}$$

(12)

The factor F_2 was found to be relatively insensitive to changes in camber so no correction was made for this factor (N = 1).

The pressure distributions of the NACA 65-010, 65-410, 65-(18)10 and 65-(24)10 compressor blade sections in cascade were calculated for $\beta = 45°$ and $\sigma = 1.0$ by use of equations (11) and (12). Good agreement between test and computed values (fig. 10) was obtained for the uncambered section. For the NACA 65-410 section, the agreement between test and calculated results was only fair, with most of the computed values too low. A similar comparison for the NACA 65-(18)10 and 65-(24)10 sections indicated generally good agreement except for the separated region between 40 and 70 percent chord (convex surface). Equation (12) appears to describe the effects of camber with acceptable accuracy.

Effect of Thickness

The thickness of the sections in cascade affects the flow over the blade surfaces because (1) the incremental velocities are a function of the thickness and its distribution and (2) the passage area and hence the average velocity are influenced by the thickness of the sections. For sections of average camber and thickness the incremental velocities due to thickness are significantly less than the increments due to camber. The possibility existed, therefore, that changes in thickness over the usual range of 6 to 15 percent chord would exhibit interblade interference similar to that exhibited by the NACA 65-(12)10 section. The effect on the average stream velocity should be accounted for in obtaining the average velocity distribution in the usual way. The surface pressures for the NACA 65-(12)06 and 65-(12)15 sections at $\beta = 60°$ and $\sigma = 1.0$ were therefore estimated by using the factors found to be suitable for the NACA 65-(12)10 section. The comparison of estimated and test pressure distributions (ref. 7) for these sections indicates reasonable

agreement (fig. 11). Laminar separation on the concave surface of the thickest section influenced the test results for this section. The extent of the region AB to which the interference factor F_1 was applied appears to be too large for the 6-percent-thick section. Insufficient information was available to determine whether this trend is general, so that no modification of the method was made to improve the agreement.

Although the agreement between test results and estimated values was not as good for these sections as for the 10-percent-thick section, suffi-cient reason to modify the values of the interference factors for the effect of thickness was not apparent.

Summary of Equations

Equations describing the separate effects of solidity, inlet angle, and camber on the interference between airfoils in cascade at design angle of attack have been obtained. These equations can be combined into single expressions for each region to which they pertain. An equation for the factor pertaining to the unconfined region AB is obtained by com-bining equations (8), (10), and (12):

$$F_1 = 1 - \left(0.97 C_{l_o}{}^{0.2}\right)(0.08 + 0.45 \sin \beta)\left(1.15\sigma^{0.71} - 0.15\sigma^3\right) \quad (13)$$

An equation applying to the confined region CD and to the concave sur-face is obtained by combining equations (9) and (11):

$$F_2 = \left(1 - 0.576\sigma + 0.14\sigma^2\right)\left(1 - 0.62 \sin^2\beta\right) \quad (14)$$

Equation (14) does not fulfill the requirement that at $\sigma = 0$ the inter-ference factor shall be unity. To satisfy this requirement, an expression involving solidity to modify the term containing $\sin^2\beta$ is necessary. No data for very low solidities are available to permit determination of a suitable exponent for this expression; therefore the value $\sigma^{0.1}$ has been inserted arbitrarily:

$$F_2 = \left(1 - 0.576\sigma + 0.14\sigma^2\right)\left(1 - 0.62\sigma^{0.1} \sin^2\beta\right) \quad (15)$$

Equations (13) and (15) have been evaluated for typical values of the pertinent cascade and section parameters. Values of the interference factor F_1 are plotted in figure 12 as functions of inlet angle for sections of several cambers. Values of F_2 for several solidities are plotted against inlet angle in figure 13.

ESTIMATING PRESSURE DISTRIBUTIONS WHEN NO CONFINED PASSAGE OCCURS

At very low solidities and high inlet angles, the relative positions of adjacent blades in cascade are such that a confined passage is not formed. In attempting to estimate surface pressures under these circumstances, several difficulties are encountered. Because of these difficulties, special treatment is required.

The first problem concerns the variation of the mean velocity through the cascade. To determine how the mean velocity varied for a particular cascade combination, the NACA 65-(12)10 section was tested at $\beta = 60°$, $\sigma = 0.50$, and $\alpha = 8.0°$. Surveys of static pressure over the flow field were made. These results are plotted in figure 14 as contours of constant dynamic pressure expressed as a ratio of the upstream dynamic pressure. An indication of how the average velocity varied through the cascade can be obtained by observing the region midway between blades. By coincidence, the line for $\frac{q}{q_1} = 1.0$ intersects a line joining the leading edges at point B halfway between blades. In the concept of flow outlined previously, the average velocity through the cascade was assumed equal to the upstream velocity at this position and upstream of this position. Downstream of point B, the values of q/q_1 are seen to decrease in a nearly linear manner with chordwise distance. Of course, the local values do not necessarily represent the average values at any chordwise station. The fact that the contours are essentially normal to the chordwise direction indicates that the average stream values are, however, not greatly different from the midpassage values. The average velocity through the cascade was therefore assumed to vary linearly from q_1 to q_2 in the region from B to E.

A linear variation of V_{av}/V_1 between points B and E and the interference factors obtained from equations (12) and (14) were used to compute pressure distributions for the NACA 65-(12)10 section for $\beta = 45°$ and $\sigma = 0.50$ and for $\beta = 60°$ and $\sigma = 0.50$ and 0.75. With these cascade combinations, no confined passage is formed. Good agreement with test values was obtained for the forward portion of the convex surfaces and for the concave surface. Toward the rear of the convex surfaces, no resemblance between computed and test results was evident.

Tuft surveys of the flow through the NACA 65-(12)10 section at $\beta = 60°$ and $\sigma = 0.50$ were made in an attempt to determine the reason for the differences. No evidence of unusually thick boundary layers or separated flow was observed. A very rapid change in direction of the streamlines from the convex surface was noted just downstream of the trailing edge. The direction of these streamlines was changed from essentially parallel to the convex surface to approximately the downstream-flow direction. The rapid curvature of the flow in this region had the effect of reducing the incremental velocity over the trailing edge of the convex surface to zero. From equation (6), the value of interference factor was found to vary linearly from F_1 at 40 percent chord to zero at the trailing edge. Pressure distributions about the NACA 65-(12)10 section at $\beta = 45°$ and $\sigma = 0.50$ and at $\beta = 60°$ and $\sigma = 0.50$ and 0.75 using this variation of the interference factor are presented in figure 15. Good agreement between calculated and test pressure distributions was obtained although it seems unusual for the curvature of the flow near the trailing edge to affect the surface pressures so far forward.

COMPARISONS FOR OTHER SECTIONS

The equations describing the variation of interference with cascade and section parameters were obtained from data for NACA 65-series sections having $a = 1.0$ mean lines. In order to determine whether the relations might be of more general use, pressure distributions were estimated for sections of other mean-line shapes and other thickness distributions. Test data were available for sections having NACA A_2I_{8b}-series or loaded-trailing-edge mean lines with NACA 65-series thickness distributions at two solidities and three inlet air angles (ref. 6). Test pressure distributions about a section having an NACA A_4K_6-series mean line, with the loading concentrated near the leading edge, and an NACA 63-series thickness distribution have been obtained for several cascade configurations.

A comparison between experimental and estimated pressure distributions for the NACA 65-$\left(12A_2I_{8b}\right)10$ section at $\sigma = 1.0$ and 1.5 for $\beta = 30°$, 45°, and 60° is presented in figure 16. Excellent agreement was obtained for the combinations $\beta = 60°$ and $\sigma = 1.0$, $\beta = 45°$ and $\sigma = 1.5$, and $\beta = 30°$ and $\sigma = 1.0$. Acceptable agreement was obtained at the other conditions.

The values estimated by the proposed method for the NACA 63-$\left(12A_4K_6\right)06$ section at $\beta = 0°$ and $\sigma = 1.0$ and 1.5 were similar in magnitude to test results over most of the surfaces (fig. 17). For both solidities, however, the estimated points were in only fair agreement with test points for the forward portion of the convex surface.

The shape of the pressure distributions estimated for NACA A_2I_{8b}-series and A_4K_6-series sections were quite similar to the test results. The proposed method, therefore, appears of general usefulness in developing improved axial-flow compressor blade sections or to complement an experimental test program.

SAMPLE CALCULATION

The calculation sheet used in estimating the pressure distribution about the NACA 65-(12)10 section at $\beta = 60°$ and $\sigma = 1.0$ is presented in table I. The values of V_{av}/V_1, which are plotted in figure 8(d), were obtained by measurement as illustrated in figure 3(b). The values of the interference factors which were obtained from equations (13) and (15) are also plotted in figure 8(d). The incremental velocities due to the camber and thickness of this section were taken from reference 2. About 4 hours were required to draw the sections, measure the passage widths, compute and plot the chordwise variation of V_{av}/V_1 and F_1, and calculate and plot the blade-surface pressure distribution.

CONCLUDING REMARKS

Surface pressure distributions of NACA 65-series compressor blade sections in cascade at low speeds have been obtained in previous investigations. In the present study, these data were analyzed to determine whether the interference between adjacent blades was systematic. A method was devised to estimate the surface pressure distribution of an airfoil section in cascade at design angle of attack, if the characteristics of the section as an isolated airfoil are known.

From the results of this investigation, the conclusion was reached that the interference between airfoils does vary in a systematic manner. The interference relations were obtained through the use of a new concept of the flow in cascade. Existing cascade data were used to find empirical values for the interference factors. For practical purposes, the variation of the interference with the relevant cascade and section parameters is expressed by simple equations. It is suggested that the concept of flow proposed herein might provide the basis for an analytical method of determining the interference relations between airfoils in cascade.

Comparisons were made between pressure distributions estimated by using the method devised in this investigation and values from cascade tests. In these comparisons the NACA 65-series compressor blade sections

and other blade sections were used. These comparisons indicated satis-
factory agreement between estimated and experimental values. This pro-
posed method appears to have general application and should be of value
to complement an experimental program or to reduce the number of tests
required in selecting improved axial-flow compressor blade sections.

Langley Aeronautical Laboratory,
        National Advisory Committee for Aeronautics,
                Langley Field, Va., June 10, 1953.

APPENDIX

Many mean-line shapes of interest in the field of turbomachines can be constructed by combining the basic mean lines presented in reference 2. However, no general method of designating such combined mean-line shapes has appeared. The following system is used herein:

Mean-line designation	a
A	1.0
B	.9
C	.8
D	.7
E	.6
F	.5
G	.4
H	.3
I	.2
J	.1
K	0

A subscript is used to specify the weighting given the basic mean lines making up a combined mean line. Thus, A_4K_6 indicates that an $a = 1.0$ mean line with $C_{l_0} = 0.4$ is combined with an $a = 0$ mean line of $C_{l_0} = 0.6$. (In general, the mean-line designation is given for a camber of $C_{l_0} = 1.0$.)

If a basic mean line is reversed or used backwards to the manner presented in reference 2, the subscript b is added to the weighting subscript. Thus, A_2I_{8b} indicates that an $a = 1.0$ mean line with $C_{l_0} = 0.2$ is combined with an $a = 0.2$ mean line of $C_{l_0} = 0.8$, and the $a = 0.2$ mean line is reversed. To clarify the meaning of these designations, the loading diagrams or resultant pressure coefficients for the mean-line types presented herein are plotted in figure 18.

Several reports describing cascade and rotor tests of compressor blade sections having $a = 1.0$ mean lines have been published. In order that no conflict may arise between present and past designations, when no letters appear to define the mean-line type, it will be assumed that an $a = 1.0$ mean line is used. When several mean-line types are discussed and conflict might arise, the $a = 1.0$ mean line will be designated A_{10}.

REFERENCES

1. Katzoff, S., and Hannah, Margery E.: Further Comparisons of Theoreti-
   cal and Experimental Lift and Pressure Distributions on Airfoils in
   Cascade at Low-Subsonic Speed. NACA TN 2391, 1951.

2. Abbott, Ira H., Von Doenhoff, Albert E., and Stivers, Louis S., Jr.:
   Summary of Airfoil Data. NACA Rep. 824, 1945. (Supersedes
   NACA WR L-560.)

3. Herrig, L. Joseph, Emery, James C., and Erwin, John R.: Systematic
   Two-Dimensional Cascade Tests of NACA 65-Series Compressor Blades
   at Low Speeds. NACA RM L51G31, 1951.

4. Felix, A. Richard, and Emery, James C.: A Comparison of Typical
   National Gas Turbine Establishment and NACA Axial-Flow Compressor
   Blade Sections in Cascade at Low Speed. NACA RM L53B26a, 1953.

5. Westphal, Willard R., and Dunavant, James C.: Application of the Wire-
   Mesh Plotting Device to Incompressible Cascade Flows. NACA TN 2095,
   1950.

6. Erwin, John R., Savage, Melvyn, and Emery, James C.: Two-Dimensional
   Low-Speed Cascade Investigation of NACA Compressor Blade Sections
   Having a Systematic Variation in Mean-Line Loading. NACA RM L53I30b,
   1953.

7. Herrig, L. Joseph, Emery, James C., and Erwin, John R.: Effect of
   Section Thickness and Trailing-Edge Radius on the Performance of
   NACA 65-Series Compressor Blades in Cascade at Low Speeds. NACA
   RM L51J16, 1951.

TABLE I.- SAMPLE CALCULATIONS FOR NACA 65-(12)10 SECTION

$$\beta = 60°; \quad \sigma = 1.0$$

①	②	③	④	⑤	⑥	⑦	⑧	⑨	⑩	⑪	⑫	⑬	⑭
Percent chord	$\frac{V_{av}}{V_1}$ (convex)	$\frac{\Delta v_c}{v_{av}}$	$\frac{\Delta v_t}{v_{av}}$	$\frac{\Delta v_l}{v_{av}}$ ③ + ④	F	⑥ × ⑤	$\frac{V_l}{V_1}$ ② (1 + ⑦)	S (convex) ⑧²	$\frac{V_{av}}{V_1}$ (concave)	$\frac{\Delta v_l}{v_{av}}$ ④ - ③	F_2 × ⑪	$\frac{V_l}{V_1}$ ⑩ (1 + ⑫)	S (concave) ⑬²
0	1.000	0.300	0.000	0.300	0.528	0.158	1.158	1.341	0.858	-0.300	-0.090	0.781	0.610
2.5	1.000	.300	.042	.342	.528	.181	1.181	1.395	.854	-.258	-.077	.788	.621
5	1.000	.300	.069	.369	.528	.195	1.195	1.428	.847	-.231	-.069	.789	.623
10	1.000	.300	.094	.394	.528	.208	1.208	1.459	.827	-.206	-.062	.776	.602
15	.995	.300	.106	.406	.528	.214	1.208	1.459	.807	-.194	-.058	.760	.578
20	.991	.300	.114	.414	.528	.219	1.208	1.459	.791	-.186	-.056	.747	.558
30	.980	.300	.126	.426	.528	.225	1.201	1.442	.748	-.174	-.052	.709	.503
40	.961	.300	.133	.433	.501	.217	1.170	1.369	.713	-.167	-.050	.677	.458
50	.938	.300	.133	.433	.449	.194	1.120	1.254	.700	-.167	-.050	.665	.442
60	.908	.300	.096	.396	.388	.154	1.048	1.098	.695	-.204	-.061	.653	.426
70	.871	.300	.055	.355	.335	.119	.975	.951	.695	-.245	-.073	.644	.415
80	.822	.300	.005	.305	.305	.093	.898	.805	.695	-.295	-.088	.634	.402
90	.775	.300	-.050	.250	.299	.075	.833	.694	.695	-.350	-.105	.622	.387
100	.716	.300	-.116	.184	.299	.055	.755	.570	.695	-.416	-.124	.609	.371

NACA
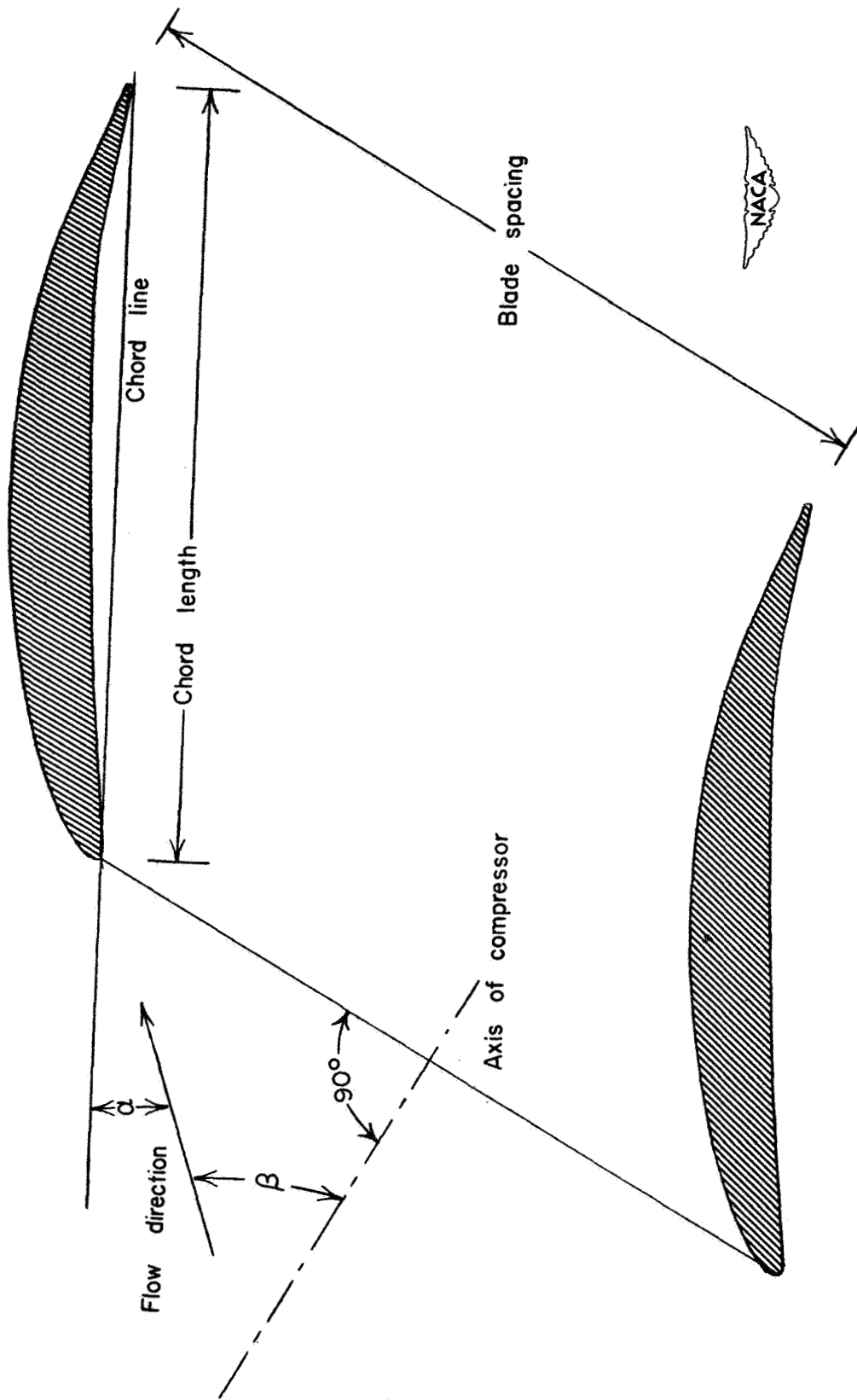
Figure 1.- Sketch illustrating symbols and nomenclature employed in this report.
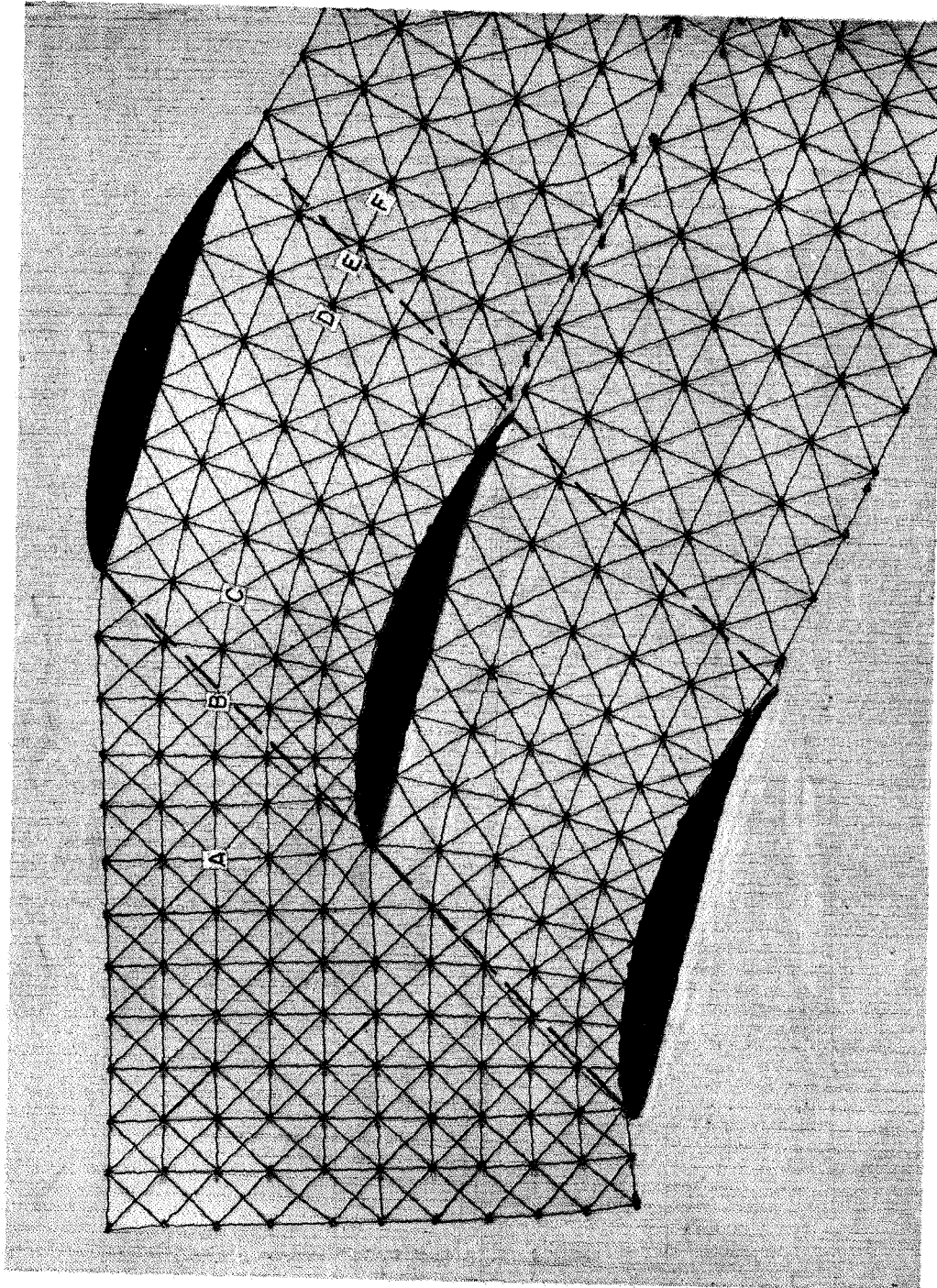
Figure 2.- Wire-mesh plot of potential flow through a typical cascade of compressor blade sections.

L-76247.1
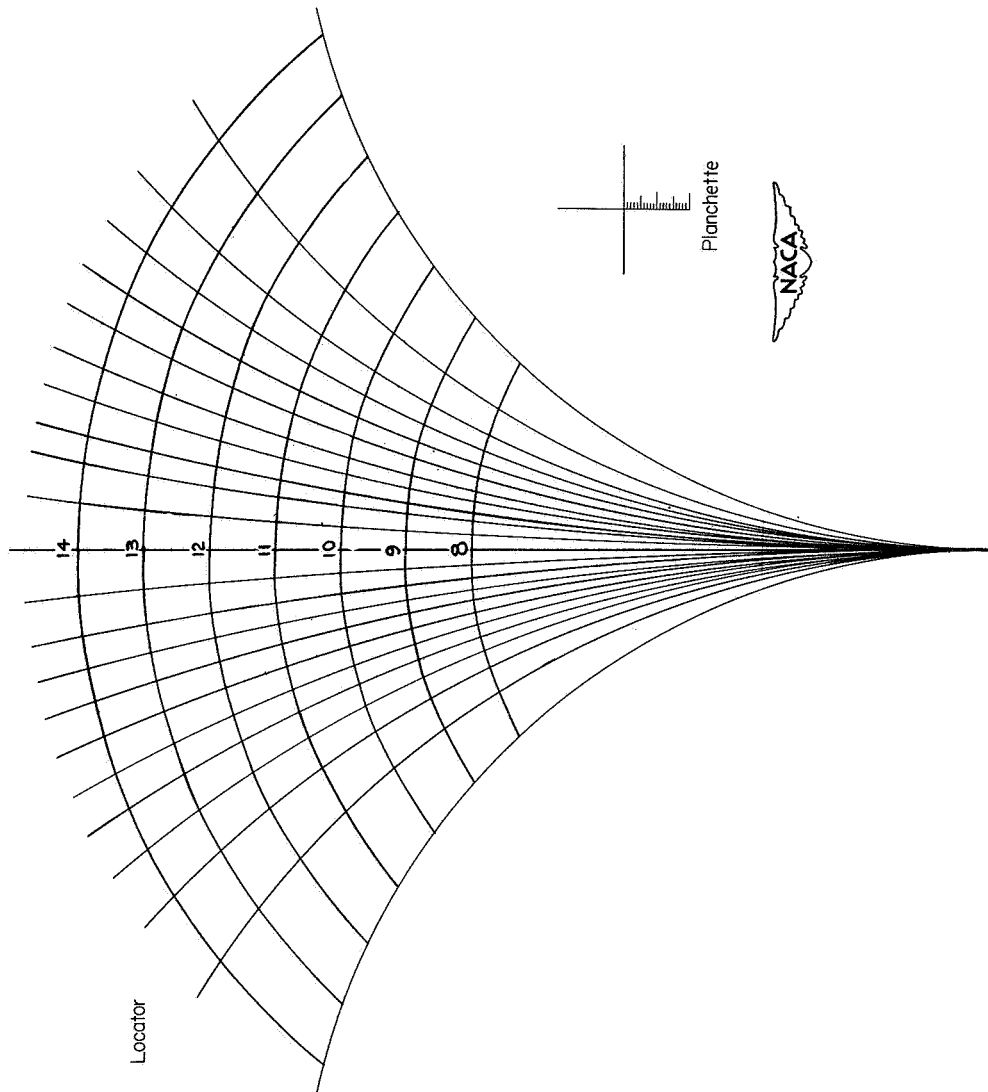
(a) Aids used to determine flow areas.

Figure 3.- Illustration of the method used in determining flow areas through blade passages.
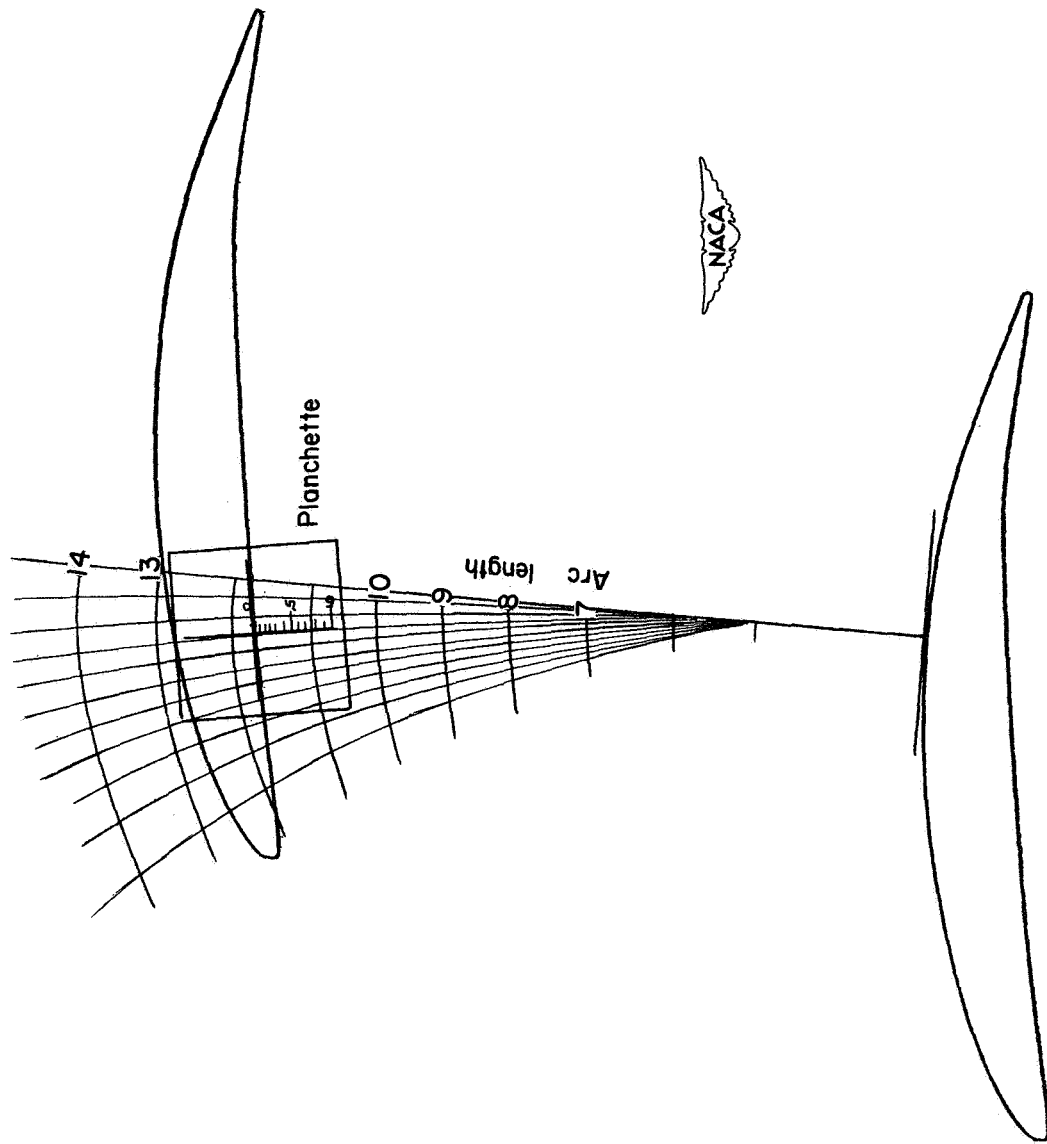
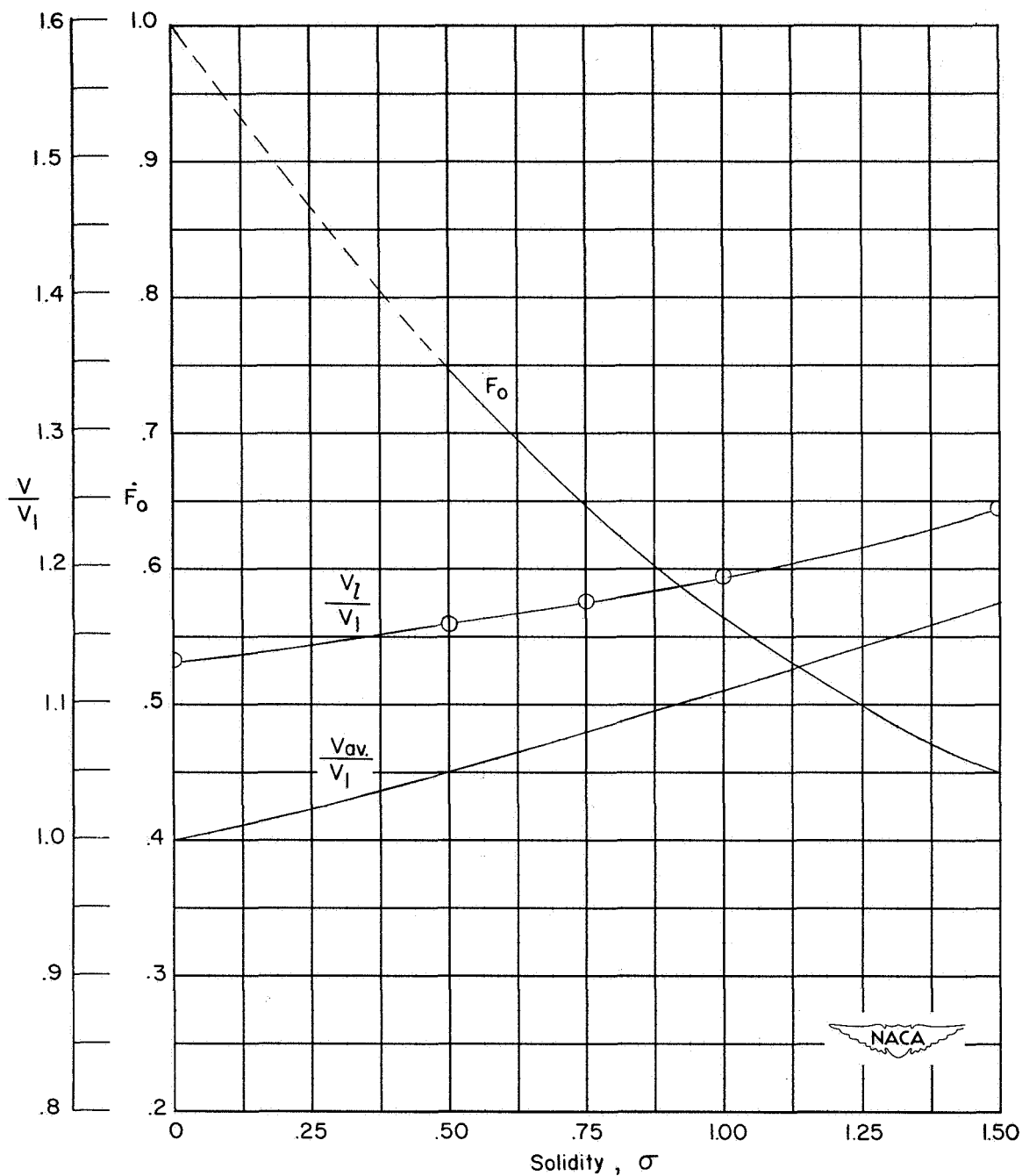(b) Use of locator and planchette.

Figure 3.- Concluded.

Figure 4.- Variation of local velocity, average passage velocity, and interference factor with solidity for the 40-percent-chord station of the NACA 65-010 section at $\beta = 0^{\circ}$.
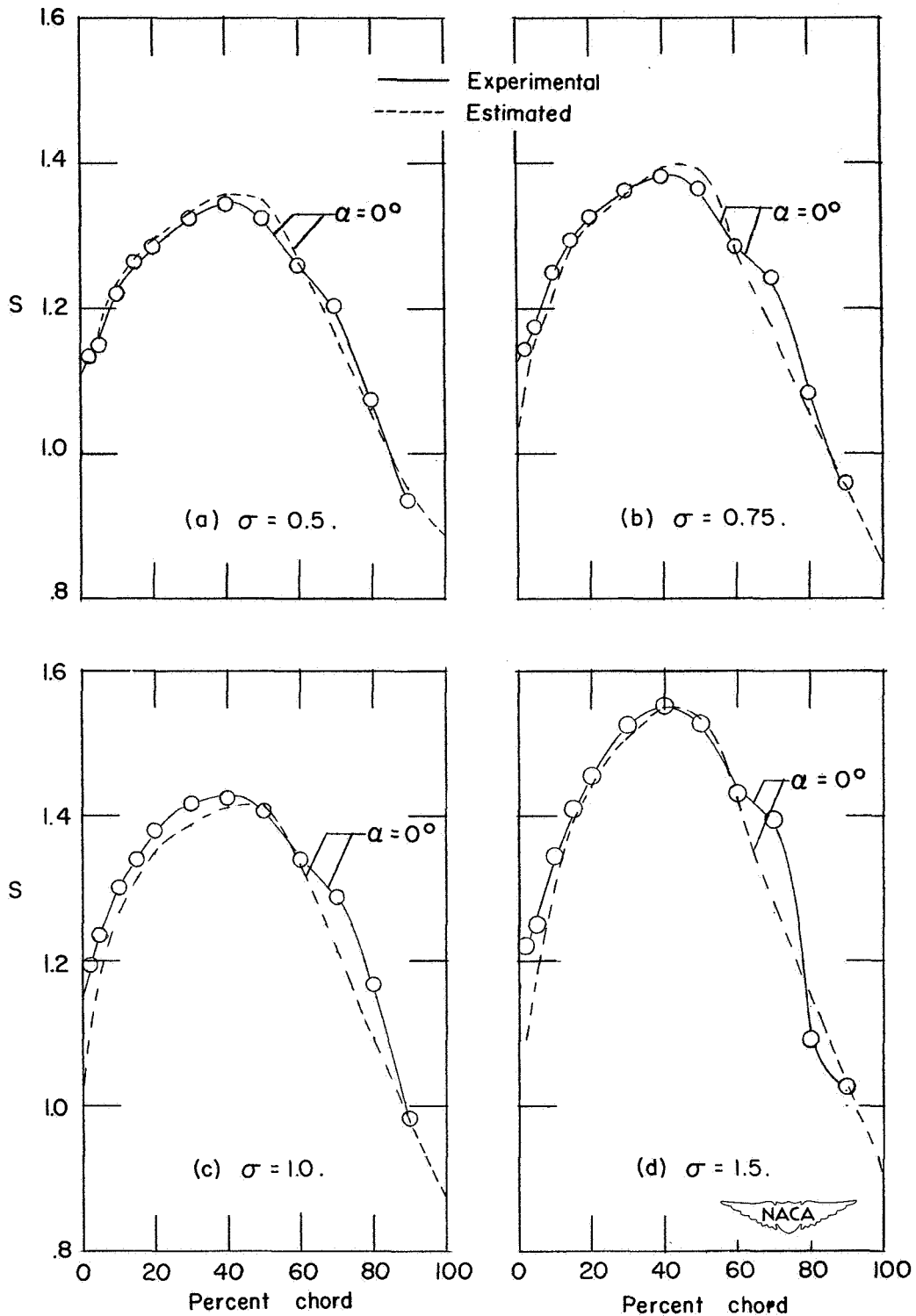
Figure 5.- Comparison of estimated and experimental pressure distributions of the NACA 65-010 compressor blade section for several solidities at β = 0°.
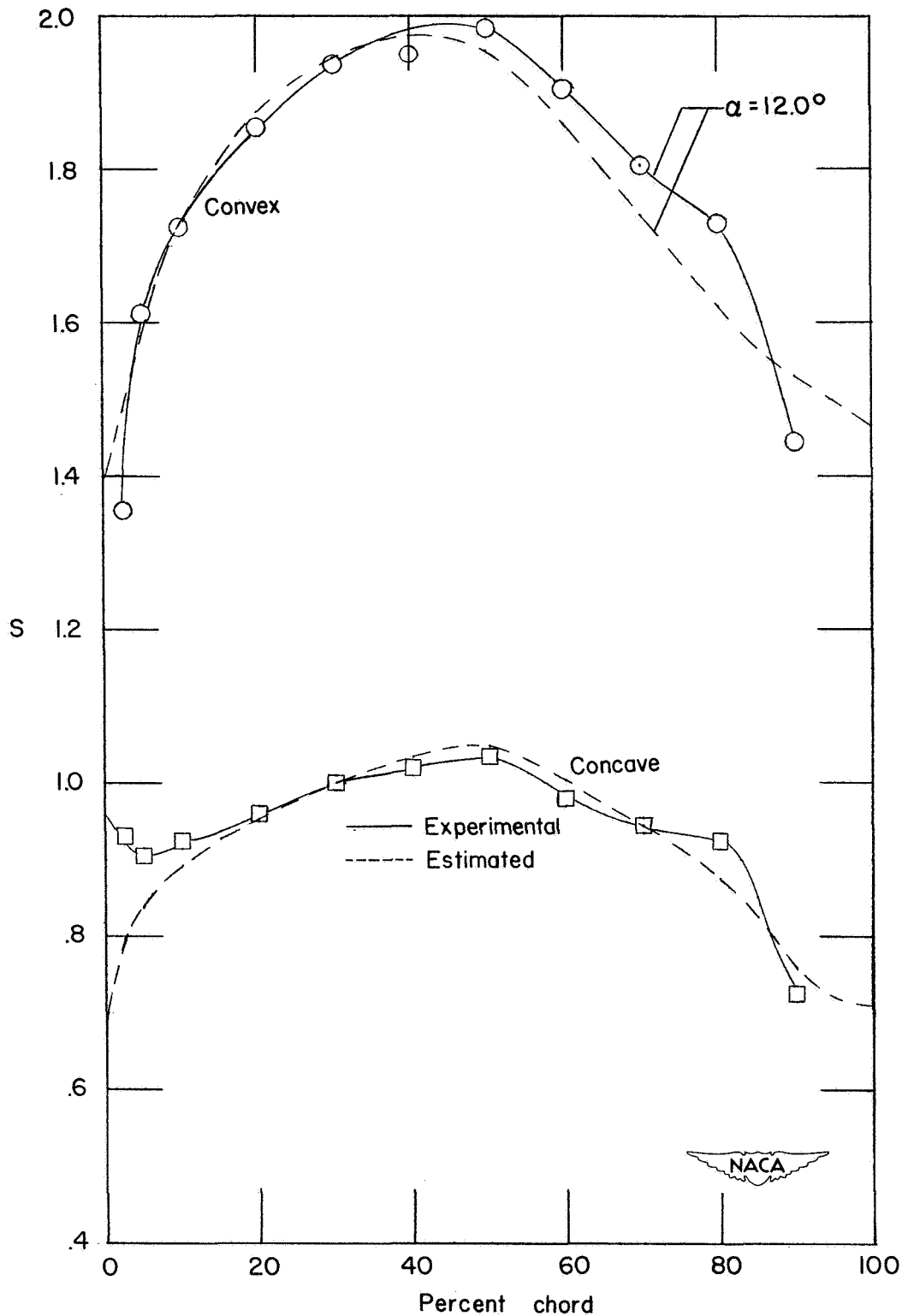
Figure 6.- Comparison of estimated and experimental pressure distributions of the NACA 65-(12)10 compressor blade section at $\beta = 0°$ and $\sigma = 1.0$.
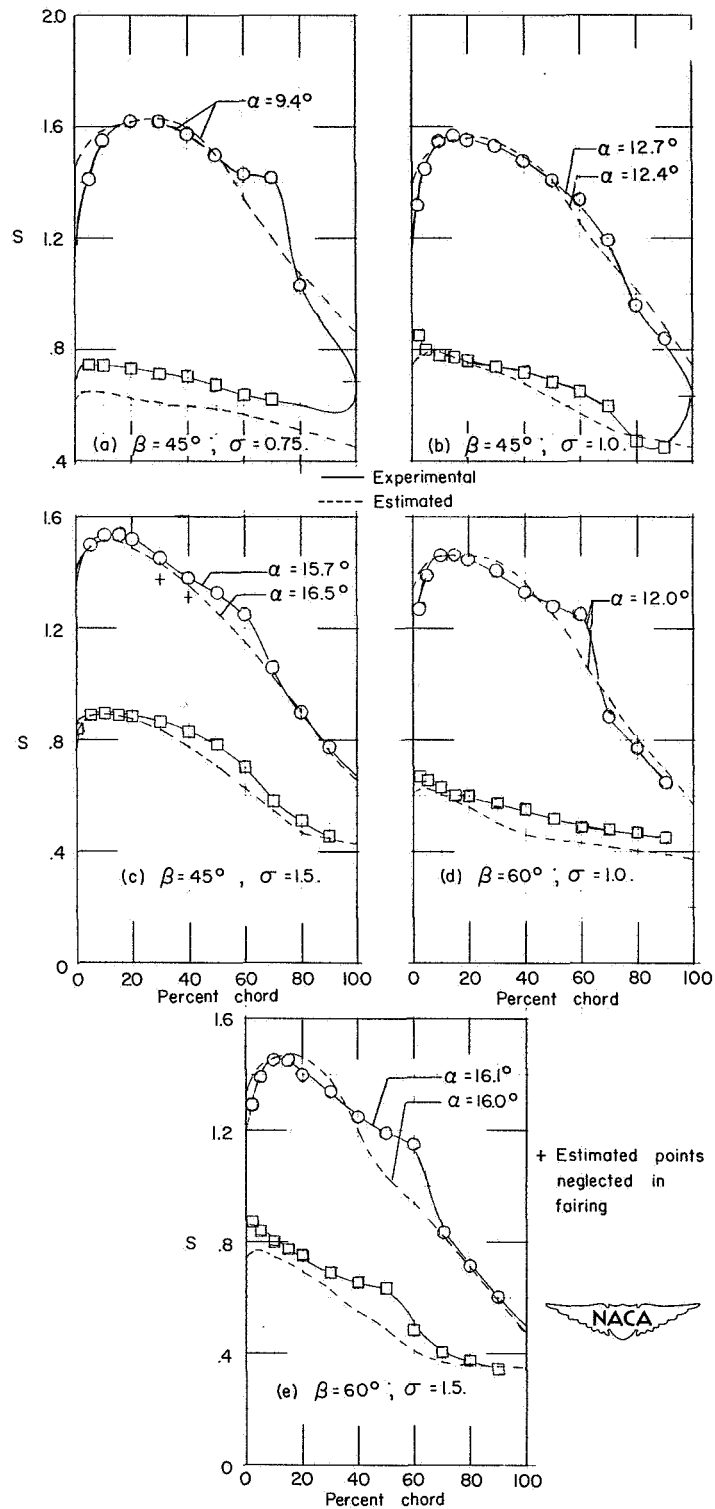
Figure 7.- Comparison of estimated and experimental pressure distributions of the NACA 65-(12)10 section for several solidities at β = 45° and β = 60°.
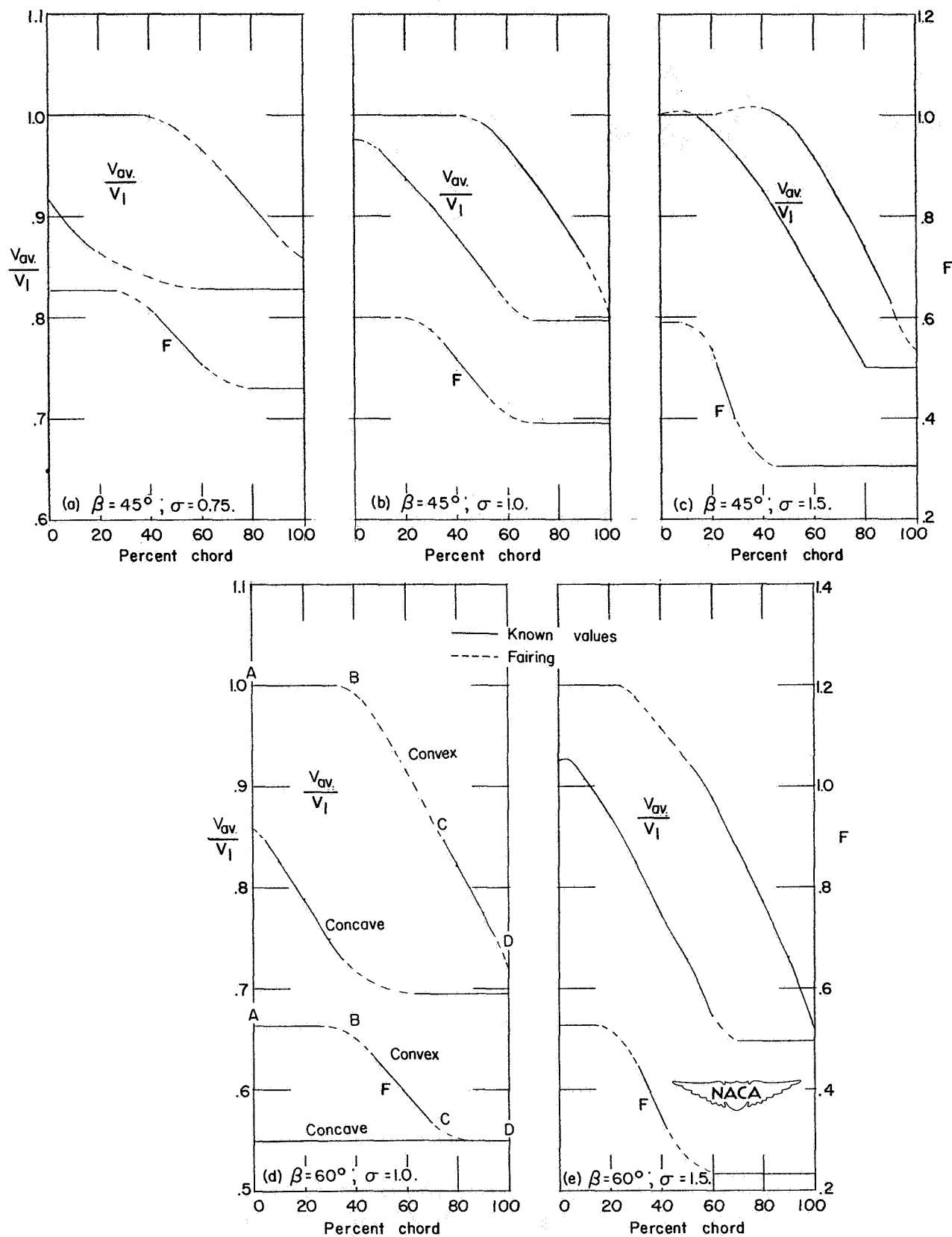
Figure 8.- Average passage velocity distributions and interference factors corresponding to the pressure distributions presented in figure 7.
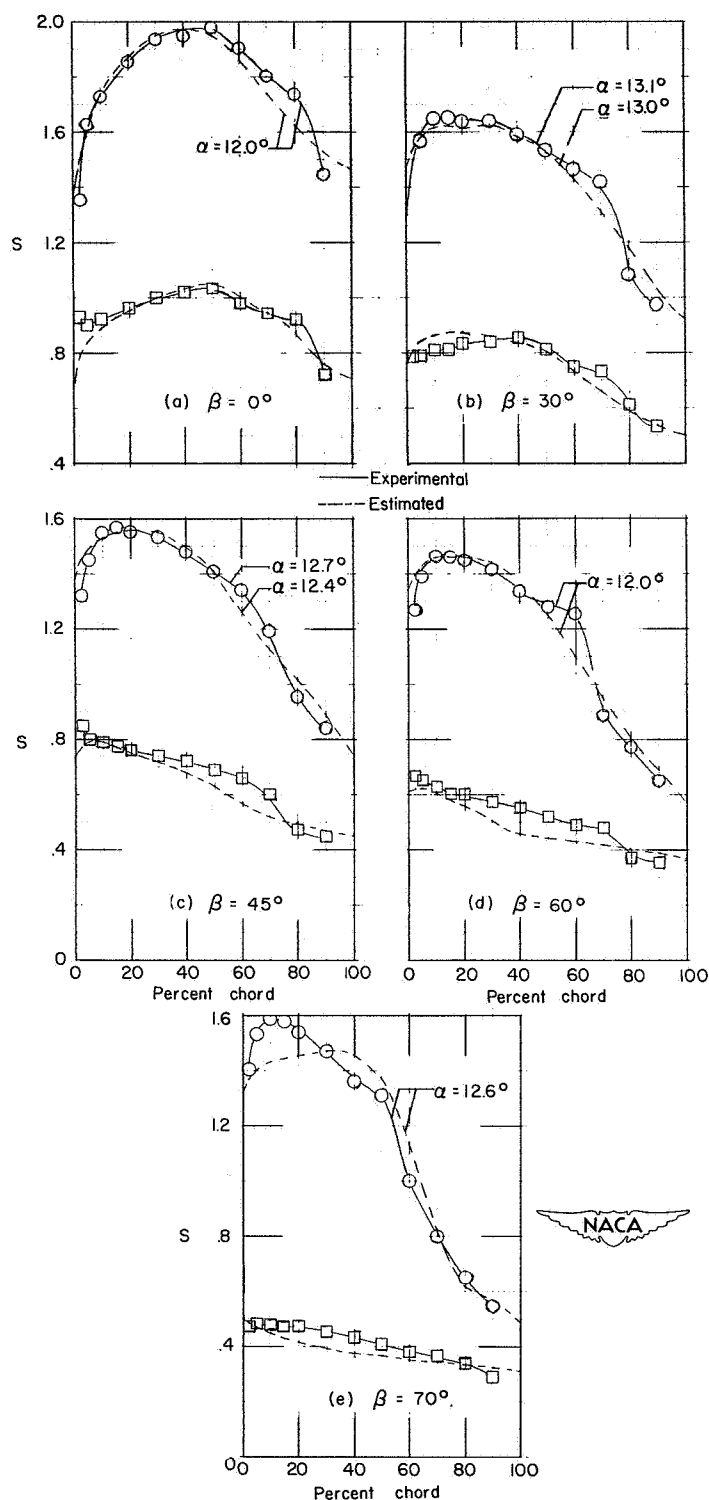
Figure 9.- Effect of inlet angle on the comparison between estimated and experimental pressure distributions of the NACA 65-(12)10 section at σ = 1.0.

32   NACA RM L53F17
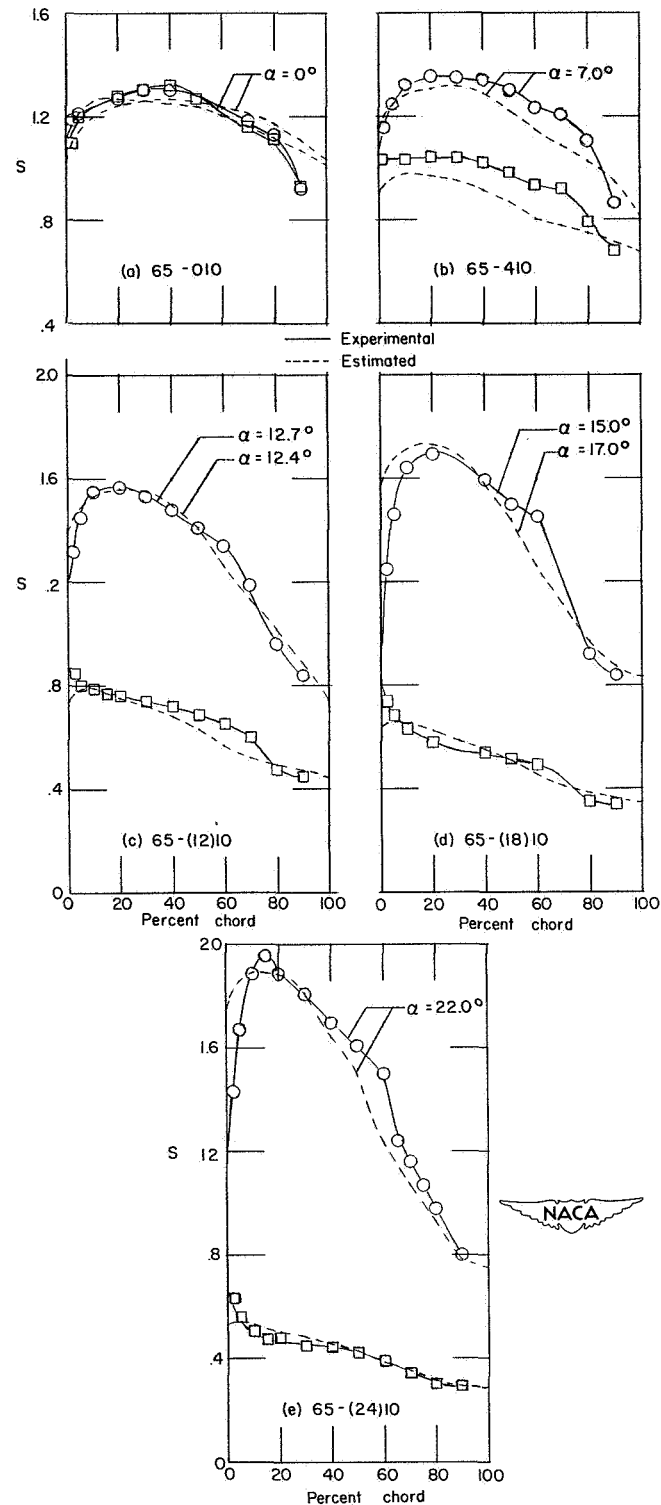
Figure 10.- Effect of camber on the comparison of estimated and
   experimental pressure distributions of NACA 65-series sections
   at $\beta = 45°$ and $\sigma = 1.0$.
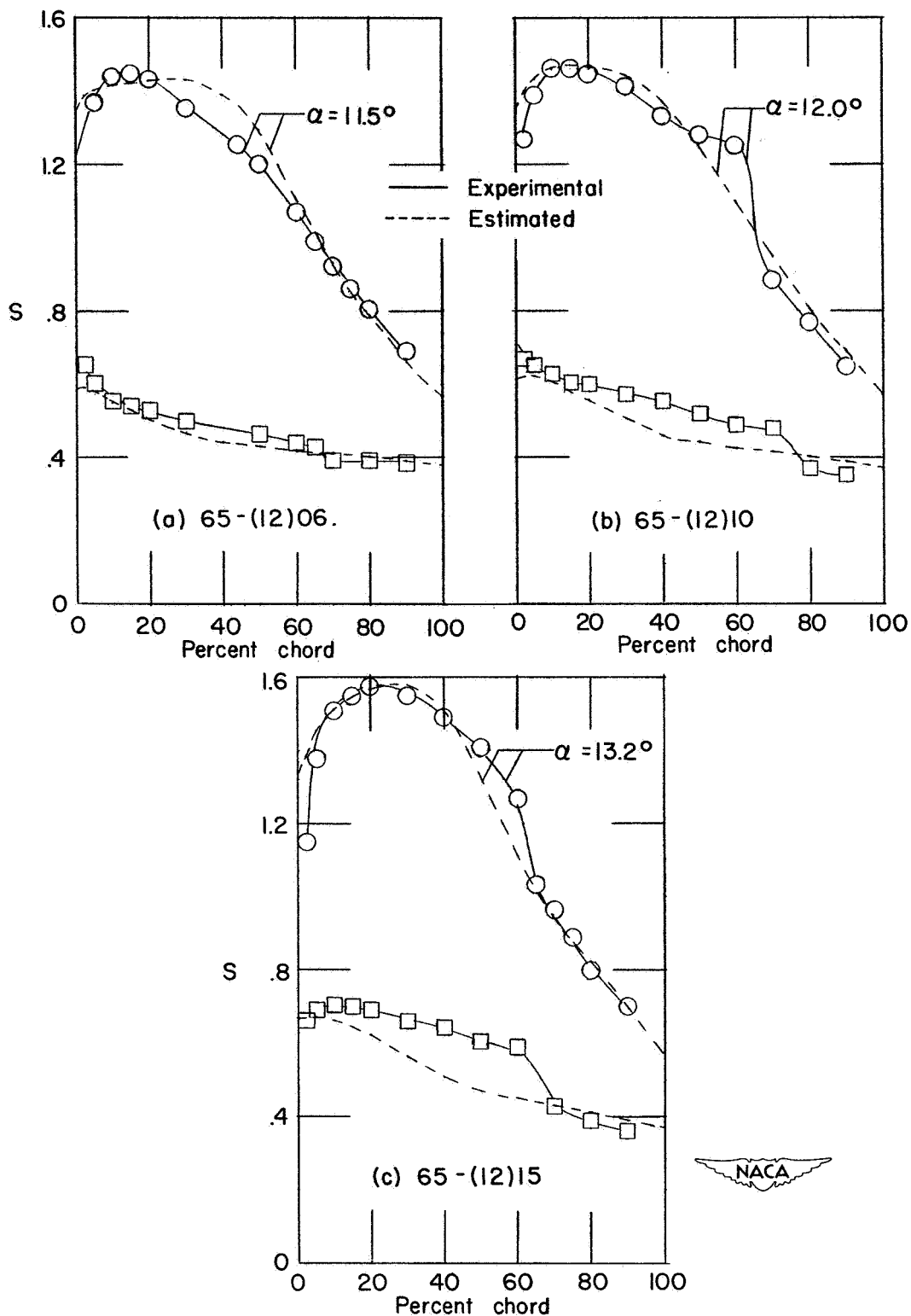
Figure 11.- Comparison of estimated and experimental pressure distributions for sections of various thickness at $\beta = 60°$ and $\sigma = 1.0$.
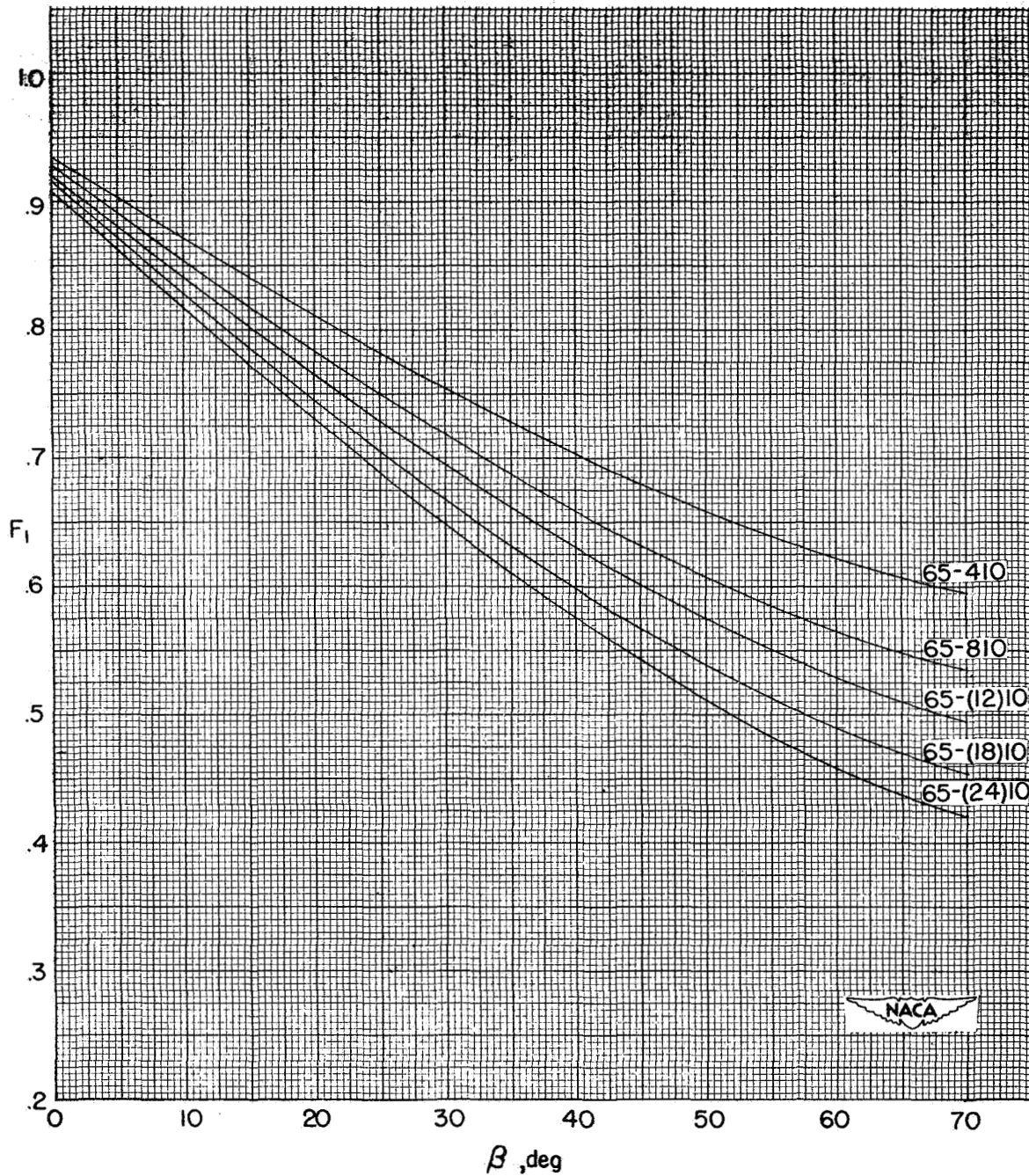
(a) $\sigma = 1.0$.

Figure 12.- Variation of interference factor F_1 with inlet angle for typical compressor blade sections.
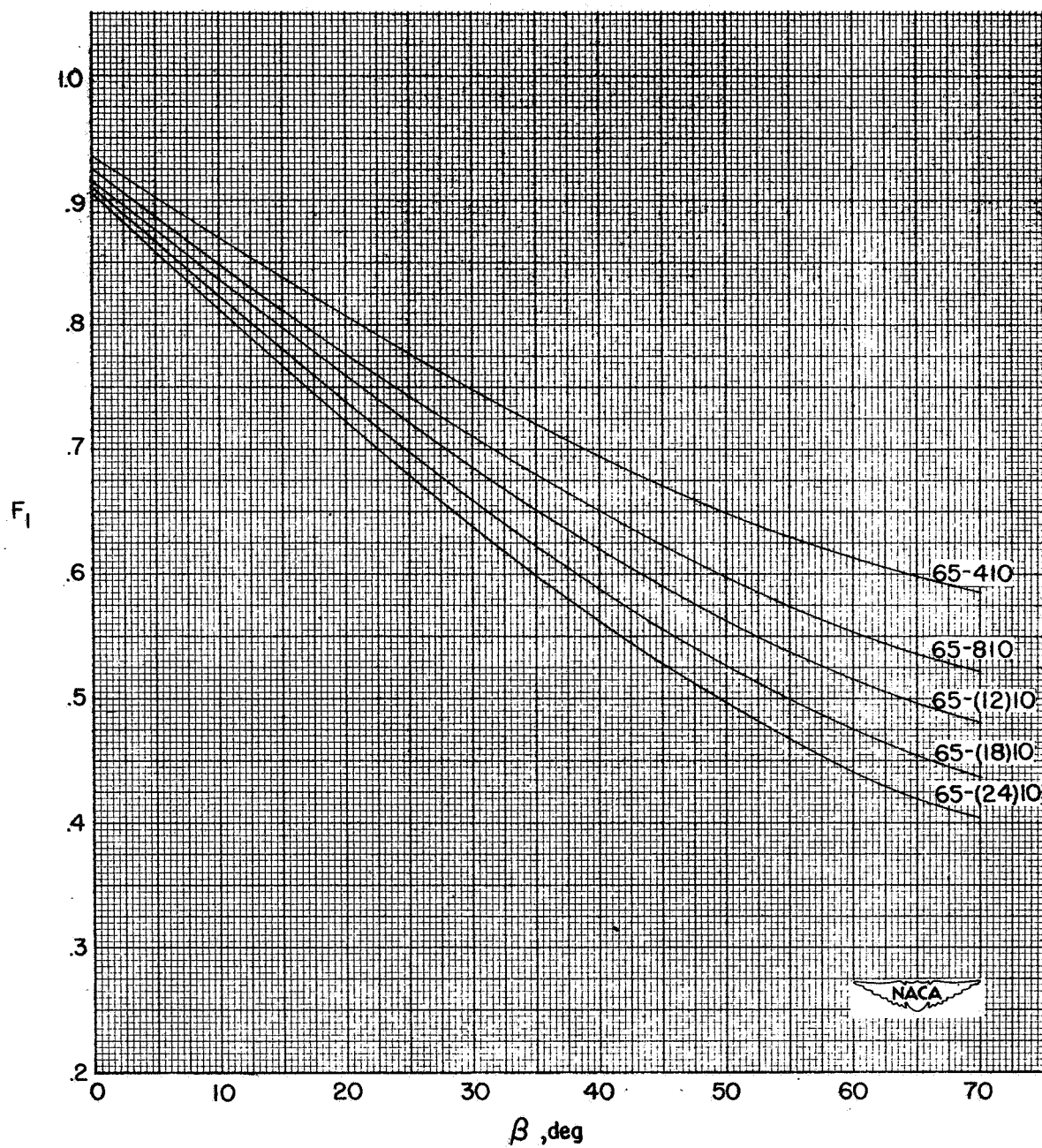
(b) σ = 1.5.

Figure 12.- Concluded.
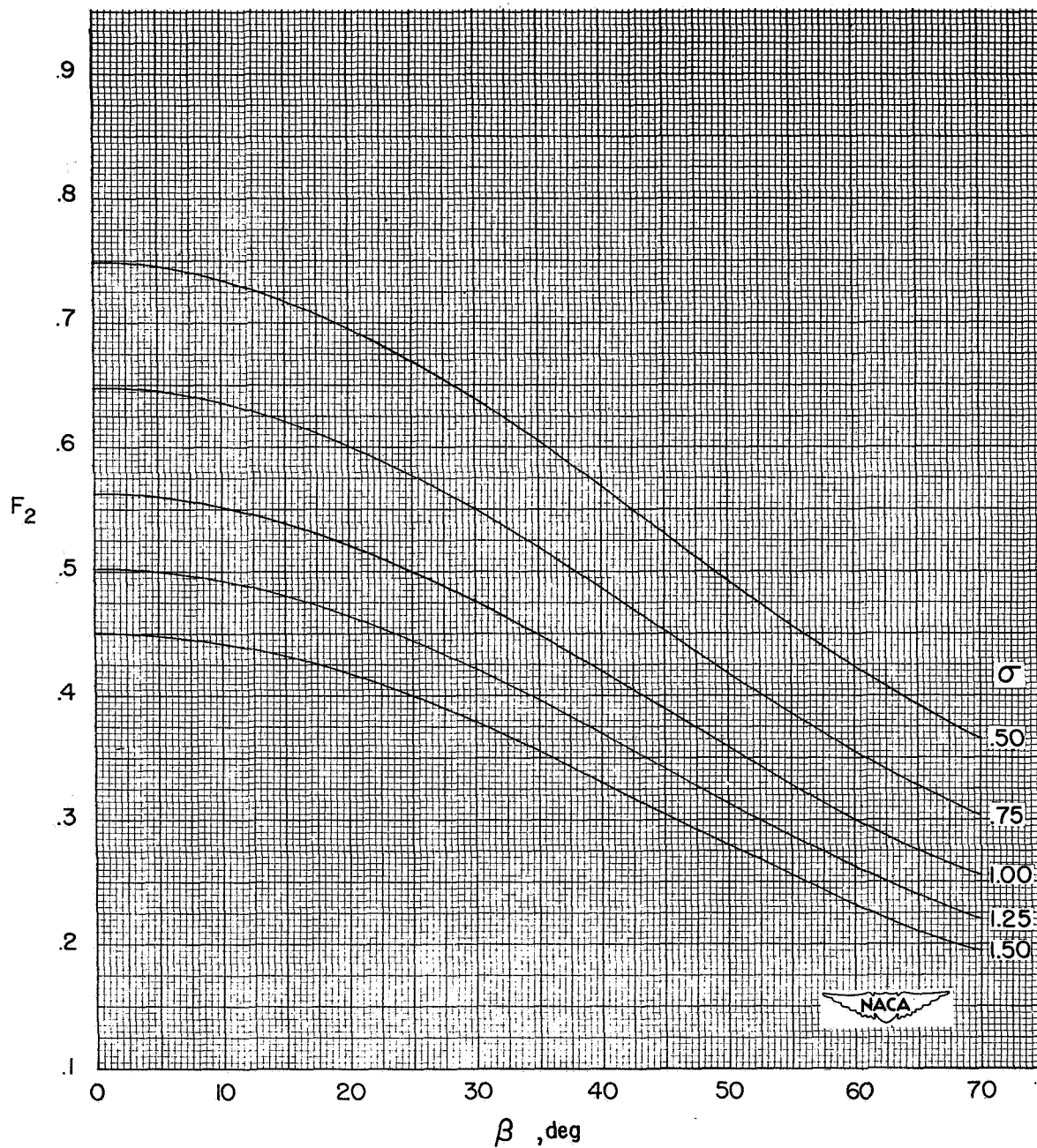
Figure 13.- Variation of interference factor F_2 with inlet angle for typical solidities.
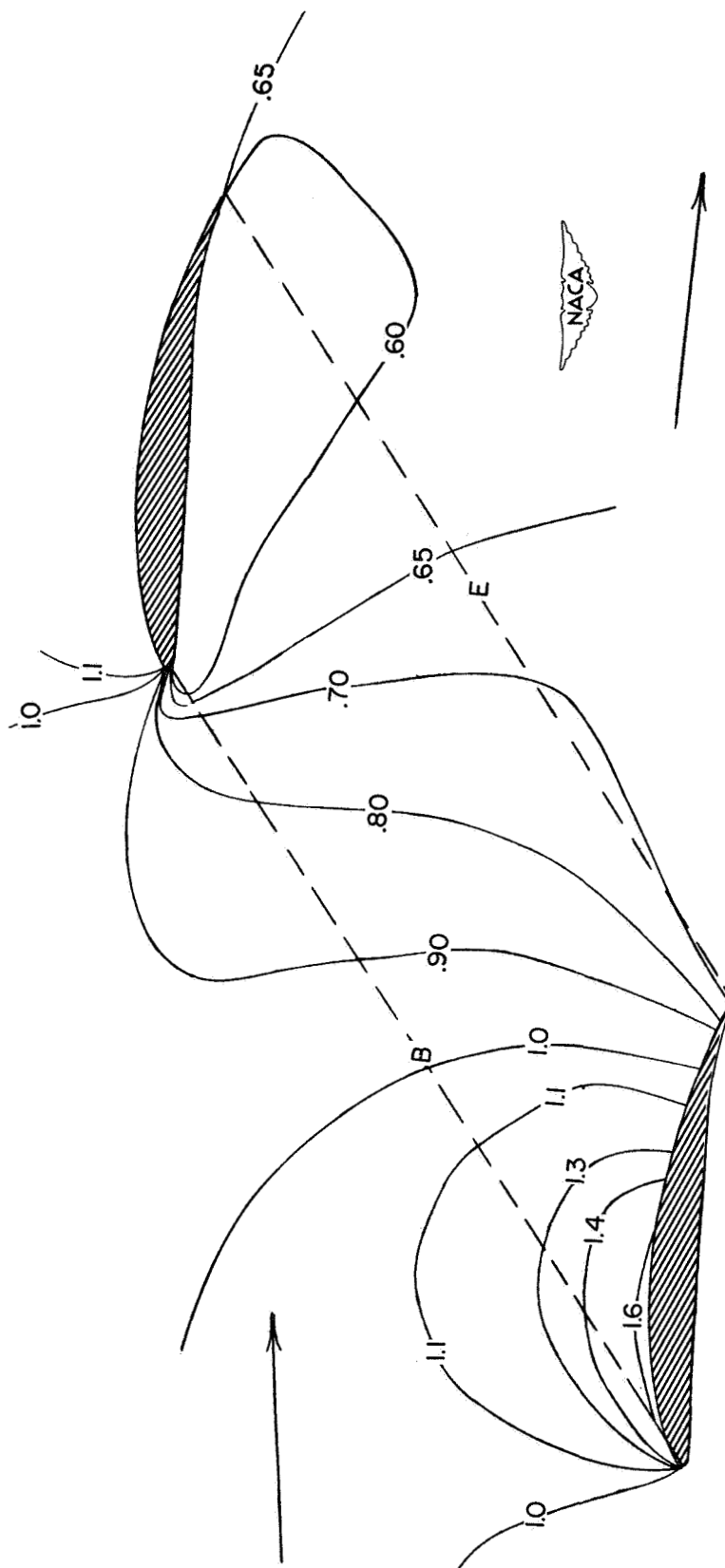
Figure 14.- The pressure distribution in the field about NACA 65-(12)10 sections at $\beta = 60°$, $\sigma = 0.50$, and $\alpha = 8.0°$.
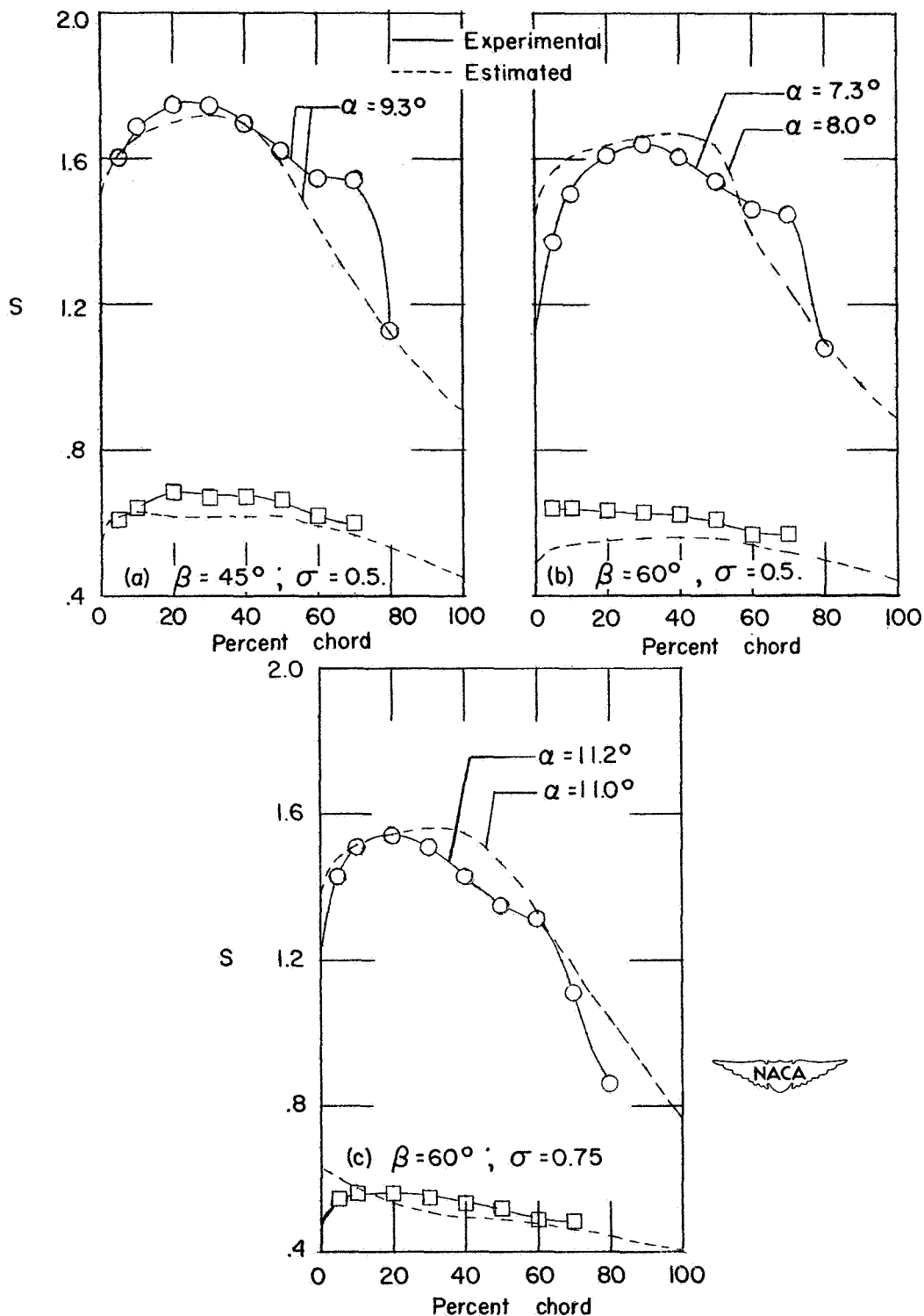
Figure 15.- Comparison of estimated and experimental pressure distributions of the NACA 65-(12)10 section at inlet angle and solidity conditions for which no confined passage exists.
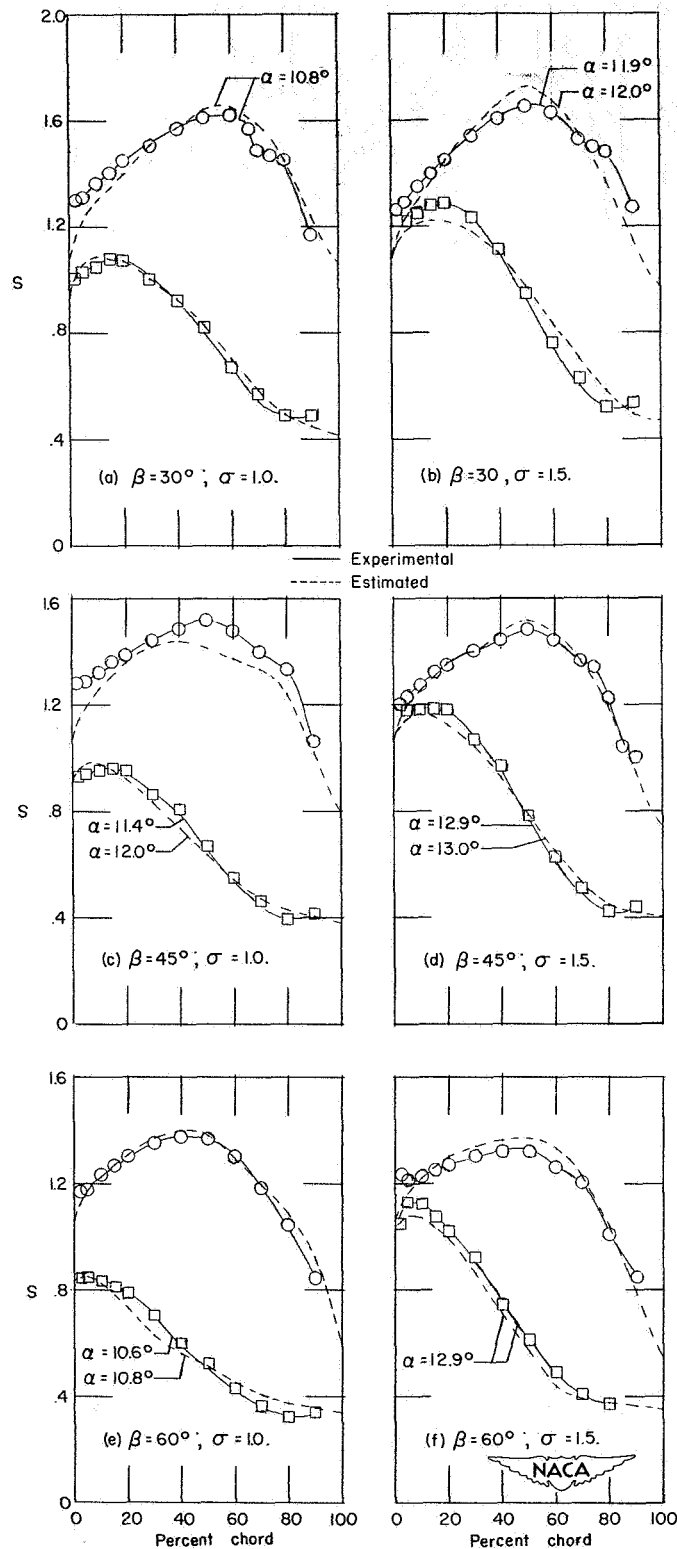
Figure 16.- Comparison of estimated and experimental pressure distributions of NACA 65-$\left(12A_2I_{8b}\right)$10 section at typical cascade conditions.
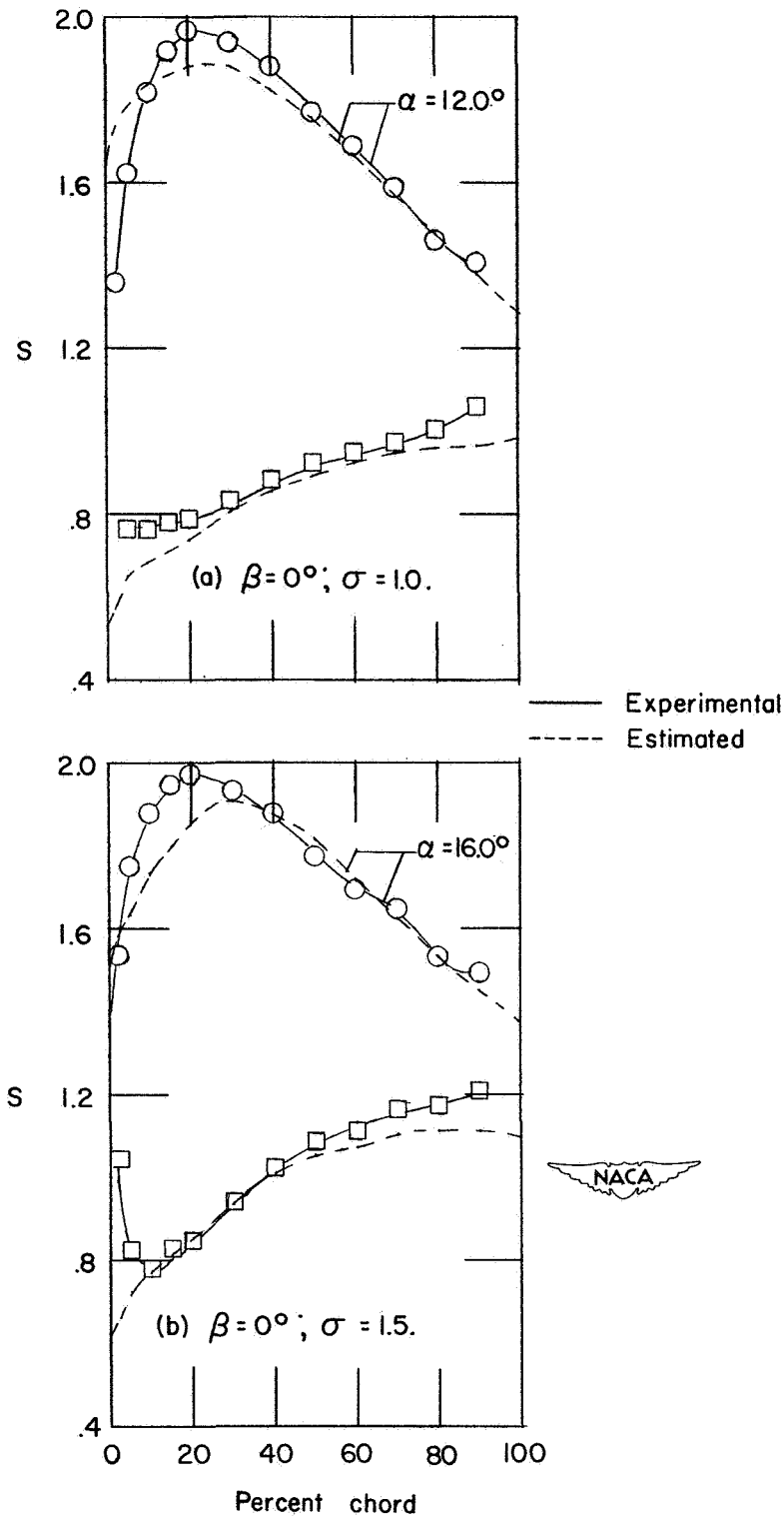
(a) $\beta = 0°$; $\sigma = 1.0$.

—— Experimental
----- Estimated

(b) $\beta = 0°$; $\sigma = 1.5$.

Percent chord

Figure 17.- Comparison of estimated and experimental pressure distributions of the NACA $63\text{-}(12A_4K_6)10$ section at $\beta = 0°$.
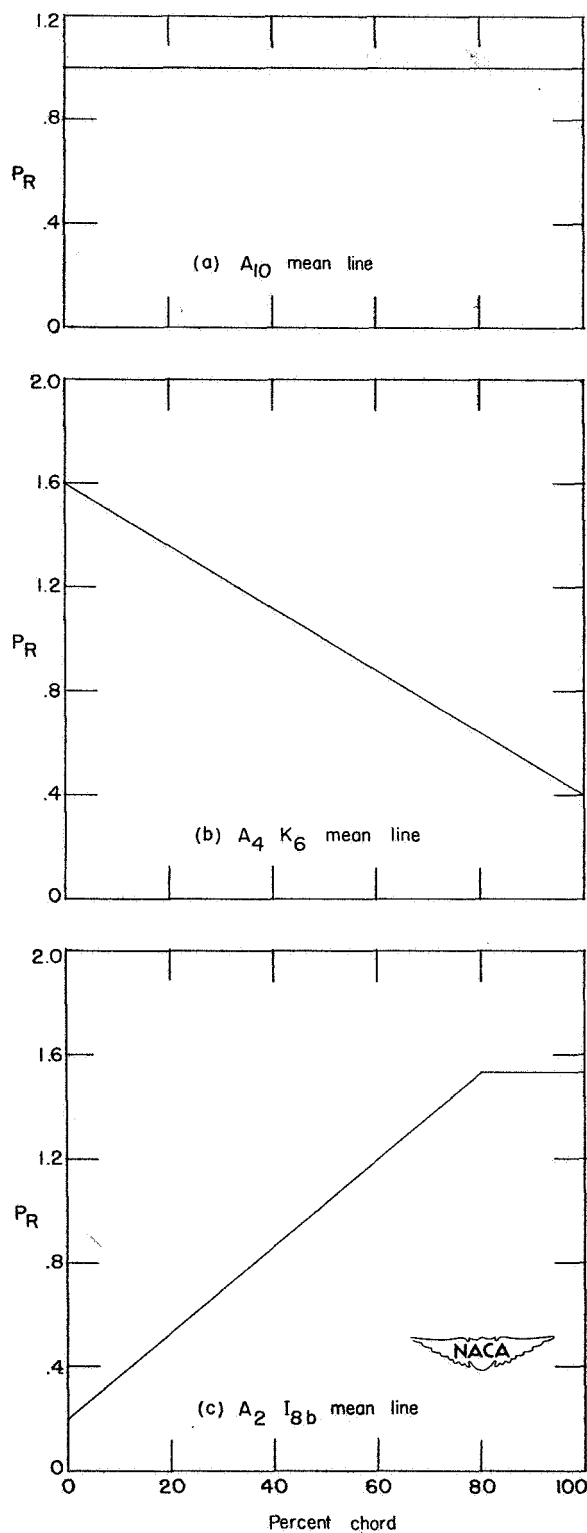
Figure 18.- Diagrams of resultant pressure coefficients for the mean-line types presented herein. $C_{l_O} = 1.0$.

UNCLASSIFIED